Copyright Warning & Restrictions

The copyright law of the United States (Title 17, United States Code) governs the making of photocopies or other reproductions of copyrighted material.

Under certain conditions specified in the law, libraries and archives are authorized to furnish a photocopy or other reproduction. One of these specified conditions is that the photocopy or reproduction is not to be "used for any purpose other than private study, scholarship, or research." If a, user makes a request for, or later uses, a photocopy or reproduction for purposes in excess of "fair use" that user may be liable for copyright infringement,

This institution reserves the right to refuse to accept a copying order if, in its judgment, fulfillment of the order would involve violation of copyright law.

Please Note: The author retains the copyright while the New Jersey Institute of Technology reserves the right to distribute this thesis or dissertation

Printing note: If you do not wish to print this page, then select "Pages from: first page # to: last page #" on the print dialog screen

ABSTRACT

HYDRODYNAMIC EFFECTS OF A CANNULA IN A USP DISSOLUTION TESTING APPARATUS 2

by
Qianqian Liu

Dissolution testing is routinely used in the pharmaceutical industry to provide in vitro drug release information for drug development and quality control purposes. The USP Testing Apparatus 2 is the most common dissolution testing system for solid dosage forms. Usually, sampling cannulas are used to take samples manually from the dissolution medium. However, the inserted cannula can alter the normal fluid flow within the vessel and produce different dissolution testing results.

The hydrodynamic effects introduced by a permanently inserted cannula in a USP Dissolution Testing Apparatus 2 were evaluated by two approaches. Firstly, the dissolution tests were conducted with two dissolution systems, the testing system (with cannula) and the standard system (without cannula), for nine different tablet positions using non-disintegrating salicylic acid calibrator tablets. The dissolution profiles at each tablet location in the two systems were compared using statistical tools. Secondly, Particle Image Velocimetry (PIV) was used to obtain experimentally velocity vector maps and velocity profiles in the vessel for the two systems and to quantify changes in the velocities on selected horizontal iso-surfaces.

The results show that the system with the cannula produced higher dissolution profiles than that without the cannula and that the magnitude of the difference between dissolution profiles in the two systems depended on tablet location. However, in most dissolution tests, the changes in dissolution profile due to the cannula were small enough to satisfy the FDA criteria for similarity between dissolution profiles (f_1 and f_2 values).

PIV measurements showed slightly changes in the velocities of the fluid flow in the vessel where the cannula was inserted. The most significant velocity changes were observed closest to the cannula. However, generally the hydrodynamic effect generated by the cannula did not appear to be particularly strong, which was consistent to dissolution test results.

It can be concluded that the hydrodynamic effects generated by the inserted cannula are real and observable. Such effects result in slightly modifications of the fluid flow in the dissolution vessel and in detectable differences in the dissolution profiles, which, although limited, can introduce variations in test results possibly leading to failure of routine dissolution tests.

HYDRODYNAMIC EFFECTS OF A CANNULA IN A USP DISSOLUTION TESTING APPARATUS 2

by
Qianqian Liu

A Thesis
Submitted to the Faculty of
New Jersey Institute of Technology
in Partial Fulfillment of the Requirements for the Degree of
Master of Science in Pharmaceutical Engineering

Otto H. York Department of Chemical, Biological and Pharmaceutical Engineering

May 2013

APPROVAL PAGE

HYDRODYNAMIC EFFECTS OF A CANNULA IN A USP DISSOLUTION TESTING APPARATUS 2

Qianqian Liu

Dr. Piero M. Armenante, Thesis Advisor — Date
Distinguished Professor of Chemical Engineering, NJIT

Dr. Laurent Simon, Committee Member — Date
Associate Professor of Chemical Engineering, NJIT

Mr. Gerard Bredael, Committee Member — Date
Associate Principal Scientist, Merck & Co., Inc.

BIOGRAPHICAL SKETCH

Author: Qianqian Liu

Degree: Master of Science

Date: May 2013

Undergraduate and Graduate Education:

- Master of Science in Pharmaceutical Engineering,
  New Jersey Institute of Technology, Newark, NJ, 2013

- Bachelor of Science in Pharmacy,
  China Pharmaceutical University, Nanjing, Jiangsu, P. R. China, 2010

Major: Pharmaceutical Engineering

This thesis is dedicated to my fiancée and parents for their love, support and encouragement.

谨以此文献给父母及挚爱的未婚夫

ACKNOWLEDGMENT

I would like to convey my gratitude to all the people who have helped me during the past eight months. First, my thesis advisor, Dr. Piero Armenante, deserves a very special acknowledgement for his consistent guidance and encouragement throughout this research work. This thesis would not have been possible without his broad and profound knowledge and moral support. I would also like to thank Dr. Laurent Simon and Mr. Gerard Bredael for participating in my committee and for their patience in reviewing the thesis.

I am particularly grateful to Ms. Bing Wang, PhD student of Chemical Engineering, for her great help and guidance in lab experiment, and her encouragement. I also appreciate the support received form Mr. Shawn W. Yetman, Mr. Yiran Zhang and Mr. Nonjaros Chomcharn.

Finally, I would like to express my deepest gratitude towards my fiancée and parents for their enormous support and inspiration. I am also thankful to all my friends who were important for the successful completion of my thesis.

TABLE OF CONTENTS

TABLE OF CONTENTS
(Continued)

LIST OF TABLES

LIST OF FIGURES

LIST OF FIGURES
(Continued)

Figure **Page**

CHAPTER 1

INTRODUCTION

1.1 Background

In the pharmaceutical industry, dissolution testing is routinely used to simulate adequate in vivo drug release of oral solid dosage forms through in vivo/in vitro correlations (IVIVC), as required by the Food and Drug Administration (FDA) and specified in United States pharmacopoeia (USP). Dissolution testing has emerged as an essential tool to guide and assess the design of new formulations, and as a quality control technique to monitor lot-to-lot consistency of the drug products.

The USP Dissolution Testing Apparatus 2 is the most commonly and widely used of all the dissolution testing devices listed in the USP (2012). It has been used in pharmaceutical industry for decades since it was first officially introduced as a USP method in the 1970s (Cohen et al., 1990). However, a review of the literature shows that it is susceptible to errors and test failures (Cox and Furman, 1982; Cox et al., 1983; Bocanegra et al., 1990; Moore et al., 1995; Qureshi and McGilveray, 1999; Qureshi and Shabnam, 2001; Mauger et al., 2003), possibly associated to the extreme susceptibility of this apparatus to small variation in its geometry and the location of the tablet during the dissolution process (Bai and Armenante, 2009).

In recent years, a number of investigations have been conducted to determine the hydrodynamics of the dissolution apparatus. Both experimental and computational methods have been used, such as Laser Doppler Velocimetry (LDV), Particle Image Velocimetry (PIV), Laser-Induced Fluorescence (LIF), and Computational Fluid Dynamics (CFD) (Bocanegra et al., 1990; McCarthy et al., 2003, 2004; Kukura et al.,

2003, 2004; Baxter et al., 2005; Bai et al., 2007, 2011; Bai and Armenante, 2008, 2009). These studies have indicated that the hydrodynamics of USP Dissolution Testing Apparatus 2 can be responsible for some of the poor reproducibility and inconsistencies of the dissolution results since the fluid flow in Apparatus 2 is highly nonhomogeneous. This system can be expected to be associated with a complex hydrodynamics, resulting in fluid velocities whose directions and intensities are highly dependent on the location within the vessel, especially at the bottom of the vessel where the tablet is usually located during dissolution testing (Bai et al., 2011).

Another source of variability during dissolution testing is associated with small changes in the geometry of the system due to the fact that USP Apparatus 2 consists of a symmetrical vessel with no baffles (Wang and Armenante, 2012). For example, a slightly irregular inner shape of a glass dissolution vessel can produce very different dissolution profiles that may result in test failures (Tanaka et al., 2005; Liddell et al., 2007). Also, Bai and Armenante (2008) reported significant changes in velocity profiles and shear rates when impeller location was placed 2 mm off center within the vessel through Computational Fluid Dynamics (CFD) approach. Such small geometry changes can be expected to affect the dissolution profile of a tablet located at the bottom of the vessel, and were confirmed by Wang and Armenante (2012) using an experimental approach (placing the paddle 8 mm off vessel's center). External vibrations have also been shown to introduce significant variability in the dissolution profiles (Gao et al., 2006; 2008).

Similarly, a sampling probe permanently inserted in the dissolution medium can also changes the symmetry of the dissolution system and the hydrodynamics within the vessel, hence possibly affecting the dissolution profile of the tablet (Wells, 1981; Savage

and Wells, 1982; Schatz et al., 2000; Bynum et al., 2001; Lu et al., 2003; Nie et al., 2009). Even if the size of the sampling probe is small, it can still act as a small baffle in a perfectly symmetrical system. The resulting loss of symmetry and the introduction of a baffling effect can result in changes in velocity profile and shear rates, which in turn could cause variations in dissolution testing results comparing to the system without such a device (Wells, 1981; Savage and Wells, 1982; Cox et al., 1984).

Cannulas are among the simplest and most common sampling probes used in Apparatus 2. A cannula consists of a thin tube attached to a syringe and used to take samples from the dissolution medium manually. Cannulas vary in length from 4.75" (120 mm) to 15" (380 mm) and are made from either stainless steel or plastic materials such as polyether ether ketone (PEEK) in order to prevent adsorption or interference with the active ingredient of the drug. A cannula is usually mounted on perforated stopper that is inserted in the vessel lid during manual sampling (to ensure that the sample is always taken at the same liquid depth) and then rapidly removed after the sample is collected. Sometimes a filter is mounted at the end of the sampling cannula. Although manual sampling is labor intensiveness and susceptibility to operator's error, it is still widely used in pharmaceutical industry and auto-sampling requires validation with manual sampling (USP 2012).

In order to simplify sample collection or to automate the sampling process, a cannula can be permanently inserted in the medium in the dissolution vessel. In such a case, the cannula can act as a small baffle and affect the system hydrodynamics and the dissolution rate just like any other probe, as already mentioned above. Investigations about the effect of sampling probes have been conducted in the past. Early studies by

Wells (1981) and Savage and Wells (1982) pointed out that the use of sampling probes, especially those larger in size, could result in appreciably faster dissolution rates than the results obtained from the system absence of a fixed probe. Cox et al. (1984) recommended using small cannulas without a filter mounted at the end to reduce hydrodynamics effects. Other investigators have instead concluded that the presence of a probe had a minimal or small effect on dissolution (Lu et al., 2003; Mirza et al., 2009; Nie et al., 2009). However, in most of those studies the effect of an auto-sampling probe, such as a fiber optic probe, was investigated. Recently, two studies on the effect of the presence of a fiber optic sampling probe on dissolution have been conducted by our group (Zhang et al, 2013; Wang et al., 2013). These studies have shown that even such a probe can alter the system's hydrodynamics significantly enough to result in small but statistically differences in dissolution profiles. However, and except as noted above, no well-defined, detailed studies with Apparatus 2 dissolution systems have been conducted in which a cannula is permanently inserted in the medium.

1.2 Objectives of This Work

The overall objective of this research work was to quantify the hydrodynamic effects of a cannula in a USP Dissolution Testing Apparatus 2. This goal was achieved here by using two different methodologies, i.e., dissolution tests using non-disintegrating tablets (salicylic acid calibrator tablets) and velocity measurements using Particle Image Velocimetry (PIV).

In order to study solely the hydrodynamic changes introduced by the cannula and its effect on the dissolution profiles, any other factors that could also affect the test results should be eliminated. As shown in previous studies (Bai et al., 2009; Wang and

Armenante, 2012) on the USP Dissolution Apparatus 2, tablets placed at different locations of the vessel's bottom produced significant variations in flow velocities and dissolution profiles. Therefore, in this study dissolution tests were conducted in the presence and in the absence of the cannula using not only tablets dropped in the vessel as recommended by the USP, but also using tablets fixed in place at 9 different positions at the bottom of the USP Apparatus 2 dissolution vessels. Statistical tools, such as f_1, f_2 factor and Student's t-values, were used to evaluate and compare the results from two systems at the same tablet location.

Additionally, PIV studies were conducted in order to find the root cause of the possible hydrodynamic effects introduced by the cannula on the dissolution profiles. PIV was used to visualize and quantify the flow velocity field in the dissolution vessel under different conditions. Then a comparison of the variations in flow field between the testing system (with the cannula) and the standard system (without the cannula) was performed. This approach also allowed a comparison to be made between changes in the dissolution profiles and variations in the flow filed that could be attributed to the presence or absence of the cannula.

CHAPTER 2

EXPERIMENTAL APPARATUS, MATERIALS AND METHODS

2.1 Dissolution Tests

2.1.1 Dissolution Apparatus

A commercial USP Dissolution Testing Apparatus 2 (Distek 5100 Bathless Dissolution Apparatus; Distek Inc., North Brunswick, NJ), as shown in Figure 2.1a, was used to conduct all dissolution experiments. This equipment can accommodate seven standard dissolution vessels consisting of unbaffled, cylindrical, hemisphere-bottomed transparent glass vessels. Each vessel is provided with a lid with two openings for sampling during in the experiments (Figure 2.1b). The agitation system consisted of a standard USP Apparatus 2 two-paddle impeller mounted on a shaft and connected to the motor in the Distek system rotating at 100 rpm.

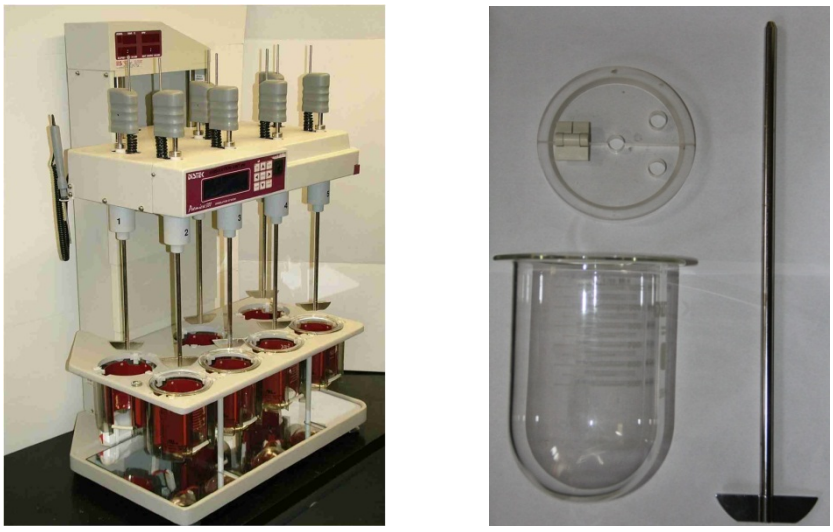

(a) (b)

Figure 2.1 (a) Distek 5100 Bathless Dissolution Apparatus **(b)** USP Dissolution Testing Apparatus 2: paddle impeller and glass vessel.

The exact geometric dimensions of the impeller were measured with a caliper, and were found to be as follows: shaft diameter, 9.52 mm; length of the top edge of the blade, 74.10 mm; length of the bottom edge of the blade, 42.00 mm; height of the blade, 19.00 mm; and thickness of the blade, 4.00 mm. The impeller clearance off the vessel bottom was 25 mm, as prescribed by the USP (2012). When the vessel was filled with 900 mL of dissolution media, the corresponding liquid height was 132.43 mm, measured from the bottom of the vessel. The geometry of the system (vessel with 900 mL of dissolution media and agitation system) is shown in Figure 2.2.

The cannula tested in this study was a bent polyether ether ketone (PEEK) cannula purchased from Hanson. The cannula was 210 mm in length (from head mount to the tail-end) with a 160-mm straight section and a 3.14-mm OD, as measured by the caliper. As specified in the USP, samples, when taken with a cannula, should be taken within a required zone in the dissolution medium, i.e., vertically midway between the top edge of the impeller and the surface of the dissolution medium, and horizontally located not less than 1 cm from the vessel wall. A stopper was used to ensure that the bottom of the cannula was located in the sampling zone during dissolution tests, although here the cannula was not used for manual sampling. The cannula with the stopper is shown in Figure 2.3 and the detailed position of the cannula in the vessel is shown in Figure 2.4.

A spectrophotometer (Cole Parmer S2100UV^{+}) was used to analyze the liquid samples and get the UV absorption data.

A pH meter (Hanna Instruments HI221) was used to adjust the pH value of the dissolution medium to 7.4 ± 0.05.

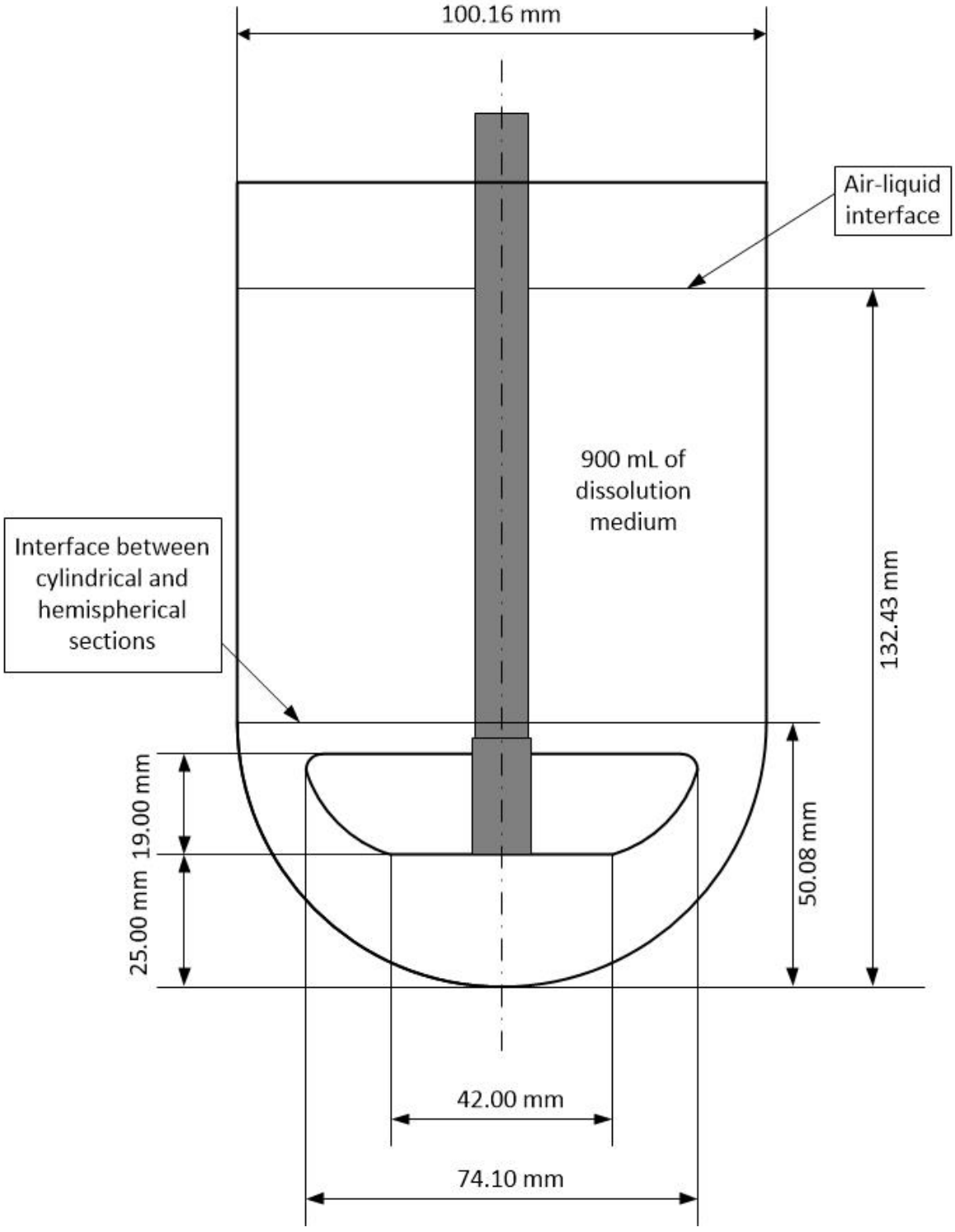

Figure 2.2 (a) Front view of USP Dissolution Testing Apparatus 2 vessel.

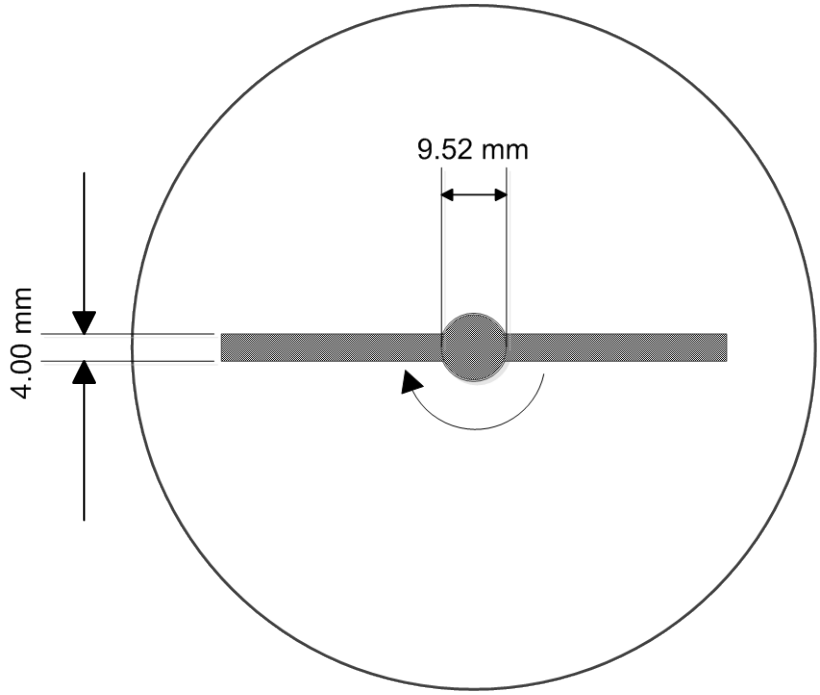

Figure 2.2 (b) Bottom view of USP Dissolution Testing Apparatus 2 vessel (Continued).

Figure 2.3 The cannula with the stopper.

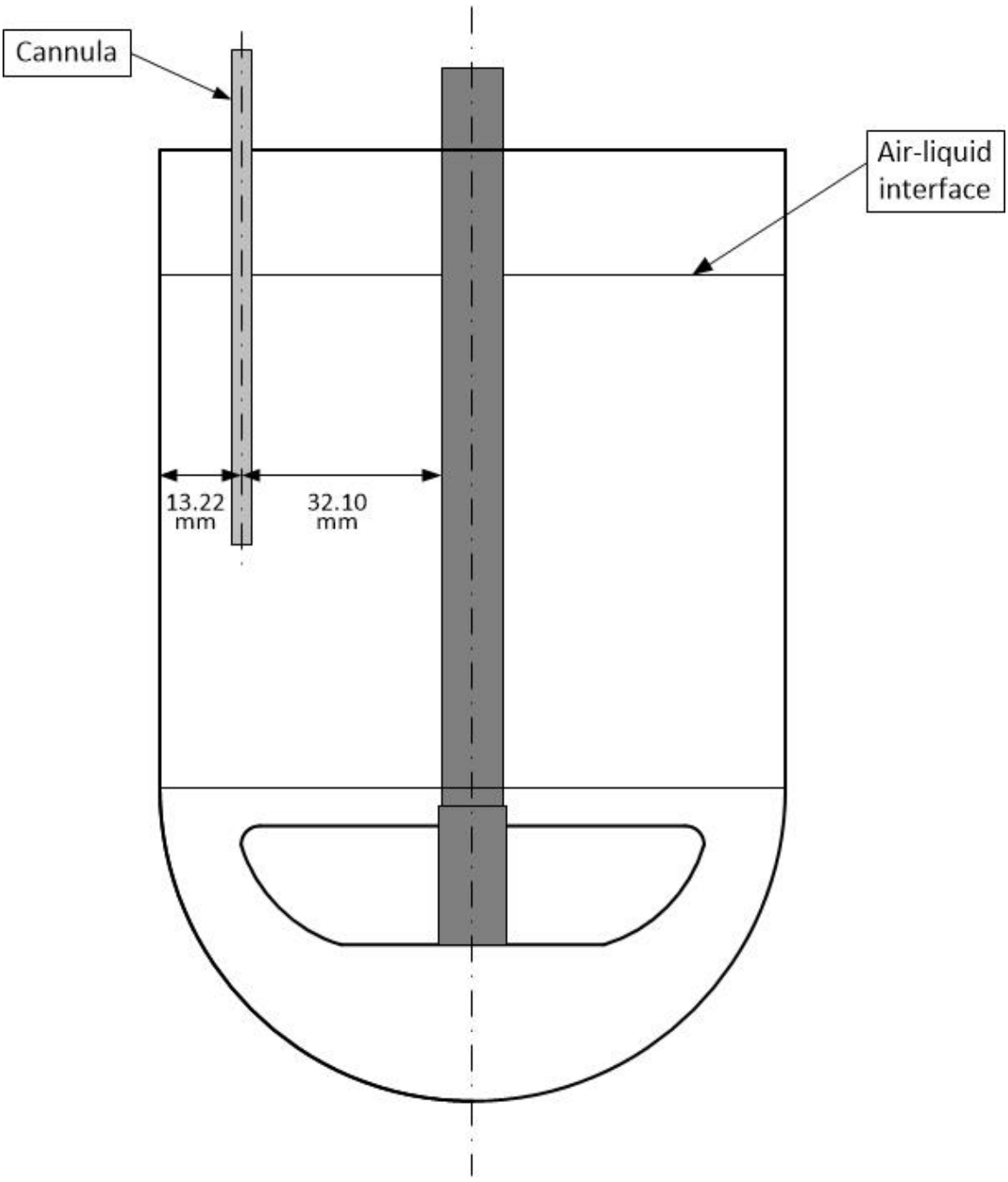

Figure 2.4 (a) Front view the dissolution testing vessel with the cannula.

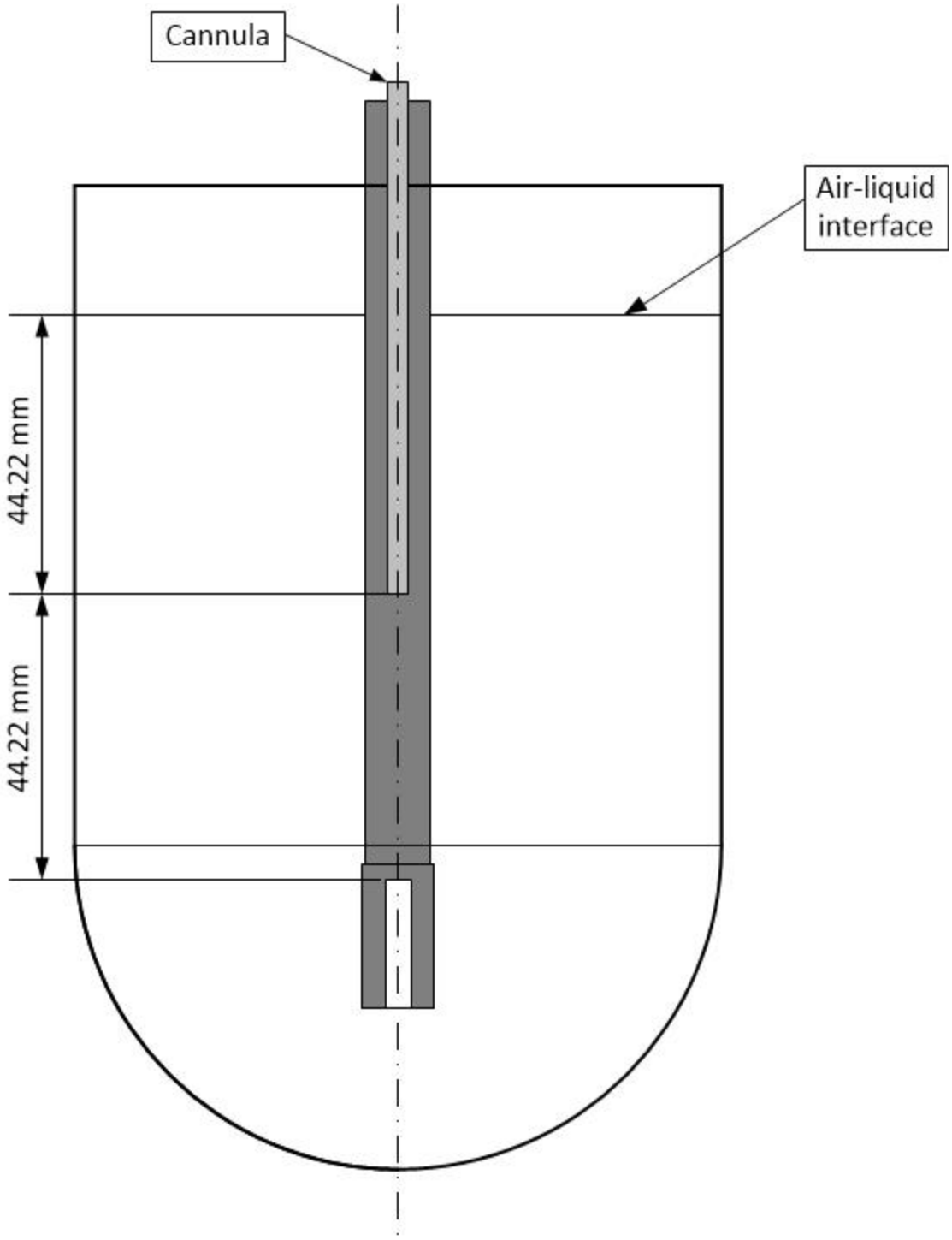

Figure 2.4 (b) Side view of the dissolution testing vessel with the cannula.

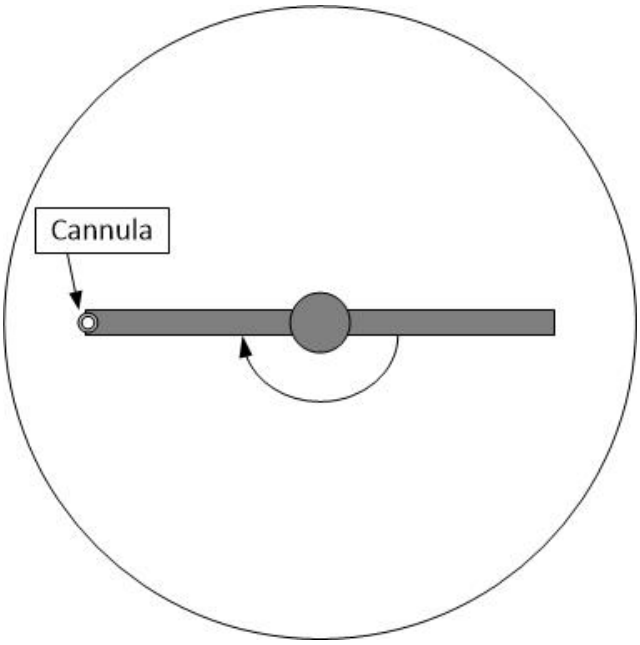

Figure 2.4 (c) Top view of the dissolution testing vessel with the cannula.

2.1.2 Dissolution Test Materials

Non-disintegrating tablets, i.e., 300 mg salicylic acid calibrator tablets (USP lot Q0D200), purchased from USP (Rockville, MD) were used in the dissolution testing experiments. A very small amount of commercial acrylic glue was used to fix the tablet at a particular position on the bottom of the dissolution vessel.

900 mL of de-aerated phosphate buffer constituted the dissolution medium. The medium consisted of a 0.05 M monobasic potassium phosphate buffer to which sodium hydroxide was added to reach a final pH value of 7.4 ± 0.05. The medium was de-aerated before using it according to the degassing method developed by Moore (1996) following the USP requirement (USP, 2012) (Figure 2.5). Accordingly, the medium was placed in a carboy tank connected to a vacuum pump. Vacuum was applied for 30 minutes while all other valves in the system were closed. This stock solution was used as needed (typically in 900 mL aliquots per test).

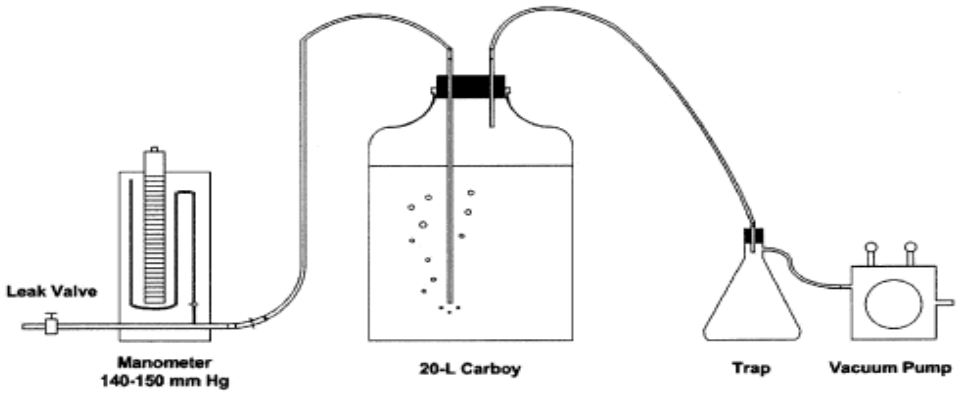

Figure 2.5 Setup of de-aeration process for dissolution medium. (USP, 2008)

In this work, two 12 mL syringes and two stainless steel cannulas (2 mm OD) were used to take samples manually from the dissolution systems. Disposable PVDF 0.45 µm filters were attached to the syringes to remove possible solid particles that could have entered the liquid samples, as described in Section 2.1.3.

2.1.3 Dissolution Test Method

Each side-by-side experiment consisted of conducting dissolution tests in both the system with the permanently inserted cannula and in the standard dissolution system without the cannula. The agitation speed was always 100 rpm and the temperature was maintained at 37 ^{o}C throughout the dissolution experiment by the system's temperature controller. Each dissolution test for any tablet configuration was performed in triplicate.

Two approaches were used to expose the tablet to the dissolution medium during the dissolution test. The first was the approach specified in the USP (2012). Accordingly, the tablet was dropped in the vessel at the beginning of the experiment, the agitation (100 rpm) was started, and the first manual sample was immediately collected.

The second approach was slightly different from that recommended by the USP in that the tablets were glued at the same predefined location on the vessel bottom in both systems with a very small head of commercial glue prior to the beginning of the experiment. Nine tablet positions were investigated in the non-symmetrical testing system with the cannula, as shown in Figure 2.6(a). Tablets in Position O were placed in the center of the vessel bottom. Positions A1, B1, C1 and D1 were all on the same inner circle 10° off-center from the vessel vertical centerline while Position A2, B2, C2 and D2 were all on the same outer circle 20° off-center from the vessel vertical centerline (Figure 2.6(b)). These angles originated from the center of the sphere comprising the hemispherical vessel bottom, and were measured starting from the vertical centerline to the point of interest, (e.g., the angle would be zero for the central point below the impeller). On each circle, the positions were spaced 90° apart from each other. In the standard system, the same nine tablet positions were selected in order to make pairs with that from the testing system, although only three positions would be sufficient in the symmetrical standard system.

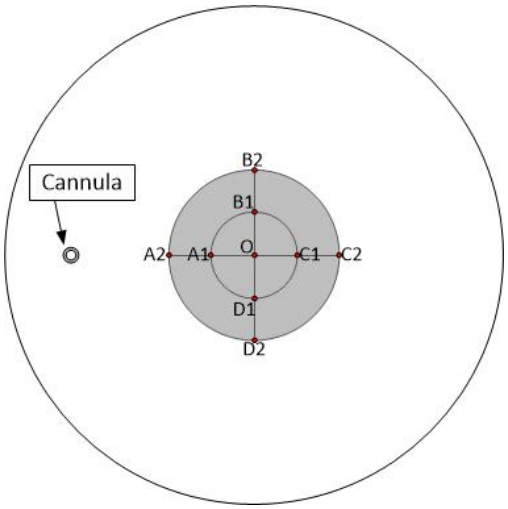

Figure 2.6 (a) Top view of the bottom of the dissolution vessel with nine different tablet positions in testing system**.**

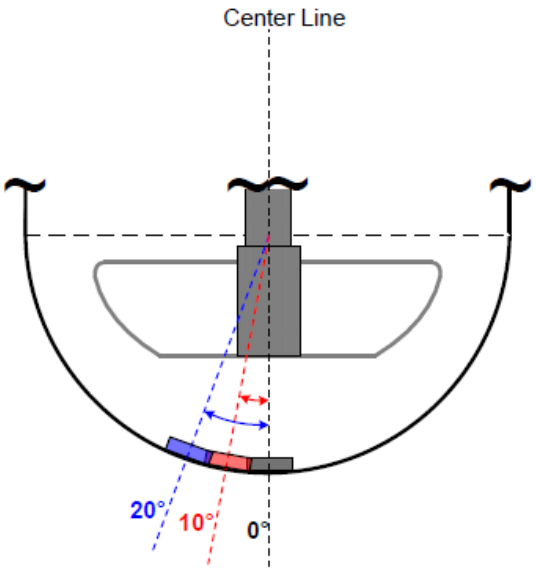

(b)

Figure 2.6 (b) The front view of the dissolution vessel with three different tablet positions (0°, 10°, 20°) in standard system (Continued).

All key geometrical measurements were checked before each experiment (impeller clearance, impeller position, etc.). Once the vessels with the attached tablets were setup properly in the Distek system, 900 mL de-aerated dissolution medium, previously preheated to 37.5 ^{o}C, was gently poured into each of the two vessels in order to minimize gas introduction and prevent the rapid initial dissolution of the tablet. The agitation was turned on immediately after the addition of the dissolution medium, the cannula was inserted to the predefined place in the testing system, and a stopwatch was started simultaneously.

Sample collection was always manual (i.e., it did not rely on the use of the cannula) and was identical for all experiments. The first pair of samples was taken immediately after starting the agitation. These samples concentrations were defined as the zero-time-point concentration. The time interval between subsequent samples was 5

minutes. Each experiment lasted 45 min, which meant that ten samples were taken for each system.

Each 10-mL aliquot sample was taken manually from the dissolution medium using a 12-mL syringe and a stainless steel cannula (2 mm OD). The volume of medium removed by sampling was not replaced, according to the USP procedure (USP, 2012). The sampling position was vertically midway between the top edge of the impeller and the surface of the dissolution medium and horizontally located 13.22 mm from the vessel wall, that is, within the USP specified sampling zone. After the sample was collected, the stainless steel cannula was removed immediately and then a disposable PVDF 0.45 µm filter was mounted on the syringe to remove possible solid particles that could have entered the sample prior the sample analysis. The initial 2 mL of each sample was discarded, and the remaining sample was transferred to a vial for further analysis.

Analysis of samples was carried out using 1-cm quartz cell placed in a UV spectrophotometer (Cole Parmer S2100UV^{+}; Cole Parmer, Vernon Hills, Illinois) measuring absorbance at 296 nm, the USP prescribed wavelength for salicylic acid. Before putting the sample solution into the quartz cell to analyze, the cell was rinsed three times with the same solution. The absorbance reading were converted to the concentration of dissolved salicylic acid using a previously obtained absorbance-vs.-concentration calibration curve (R^2=0.9998). This calibration curve was obtained by preparing reference standard solutions of salicylic acid and diluting them to obtain solutions of different known concentrations. The absorbance of these solutions generated an absorbance versus concentration standard curve.

Note that for the salicylic acid tablet, for most experiments, samples collected after t=25 minutes needed to be diluted so that their UV absorbance was in the appropriate range. These samples were diluted into one-half with dissolution medium. Additional details of the operating conditions are summarized in Table 2.1.

Table 2.1 Operating Conditions for Dissolution Experiments with Calibrated Salicylic Acid Tablet

Salicylic Acid Tablet	Operating Conditions
Dose	300 mg
Medium	900 ml de-aerated, pH=7.4 buffer (KH_2PO_4)
Temperature	37 ^oC
Agitation Speed	100 rpm
Filter	PVDF 0.45 μm
UV Wavelength (UV Spectroscopy)	296 nm
Time	5 min sampling interval; 45 min total
Sample Volume	10 ml
Sample Replacement	No

2.1.4 Dissolution Test Data Analysis

The dissolution profiles are presented in terms of drug release fraction (m_D/m_T), that is, the mass of released drug in the dissolution medium at any time *t* out of the total mass of drug initially in the tablet, as a function of time. The absorbance data obtained from the UV spectrophotometer was first converted to salicylic acid concentration at given time, (C_j, in mg/mL), and then transformed into drug mass release fraction (m_D/m_T) using the following equations, in order to account for the drug mass removed with each sample:

$$\frac{m_D(t_1)}{m_T} = \frac{C_1}{C^*} \qquad for\ j = 1 \tag{2.1}$$

$$\frac{m_D(t_j)}{m_T} = \frac{C_j}{C^*}\left[1-(j-1)\frac{\Delta V}{V}\right] + \frac{\Delta V}{V}\sum_{k=1}^{j-1} C_k \qquad for\ 2 \le j \le n \tag{2.2}$$

where j is an index identifying the number of sampling (j=1, 2, … 10), $m_D(t_j)$ is the mass of released salicylic acid at time t_j, m_T is the total mass of salicylic acid initially in the tablet, C_j is the dissolved salicylic acid concentration in the j^{th} sampling at time t_j, C^* is the concentration of salicylic acid when the tablet is fully dissolved in 900 mL dissolution medium, ΔV is each sampling volume (10 mL) and V is the initial volume of dissolution medium (900 mL). At the beginning of the experiment (t=t_1=0 minutes) the first sample was taken immediately (j=1) resulting in an initial concentration C_1, and the 10th sample was taken at t_{10}=45 minutes (j=10).

The dissolution profiles obtained with tablets at each position in the testing system were compared to those from its paired standard system in order to determine whether these dissolution curves were statistically similar or not. Two approaches were used. The first approach was that recommended by the FDA to quantify the similarity/difference of two dissolution profiles. This approach consists of a model-independent method based on the difference factor (f_1) and similarity factor (f_2) proposed by Moore and Flanner (1996):

$$f_1 = \frac{\sum_{t=1}^{n}\left|R_t - T_t\right|}{\sum_{t=1}^{n} R_t} \times 100 \tag{2.3}$$

$$f_2 = 50\log_{10}\{[1+(\frac{1}{n})\sum_{t=1}^{n}(R_t - T_t)^2]^{-0.5}\times 100\} \quad (2.4)$$

where R_t is the reference assay at time t (i.e., the results from the standard system), T_t is the test assay at the same time (i.e., the paired results from the testing system), and n is the number of time points. The difference factor (f_1) calculates the percent (%) difference between the two curves at each time point and measures the relative error between two curves. The higher the f_1 (which can be in the range of 0 to 100), the higher the average difference between reference and test curves is (Moore and Flanner, 1996). The similarity factor (f_2) is a logarithmic reciprocal square root transformation of the sum-squared error of differences between the reference and test profiles over all time points (which can be in the range -α to 100). The higher the f_2, the lower the average difference between reference and test curves is (Costa and Lobo, 2001). Public standards have been set by FDA for f_1 and f_2 factors. Accordingly, statistical similarity between the two curves being compared requires that $0<f_1<15$ or $50<f_2<100$ (FDA, 1997).

The second approach was the standard Student's t-test based on the analysis of variance and the calculation of the probability that the two sets of data came from the same underlying population (null hypothesis) using the following equations (Lapin, 1975):

$$T\text{-}value = \frac{\overline{X_D} - \mu_0}{S_D / \sqrt{n'}} \quad (2.5)$$

$$DF = n' - 1 \quad (2.6)$$

where $\overline{X_D}$ is the sample mean (here is the average differences between two curves), μ_0 is the population mean (in this case the constant from which to test whether the average of the difference is different, i.e., μ_0=0 here), S_D is the sample standard deviation (here is the standard deviation of the differences between curves), *DF* is the degree of freedom (here the initial data point at t=0 was not used) and *n'* is the number of samples excluding the first one (Schatz et al., 2001). The probability that the null hypothesis is correct can be obtained from the T-value in Equation (2.5) using the experimental data as input and with the table of values from Student's t-distribution (Lapin, 1975). The significance level was chosen here to be 0.05, i.e., if the probability obtained was smaller than 0.05, the null hypothesis was rejected and the two groups of data were considered to be statistically different.

2.2 Particle Image Velocimetry (PIV)

2.2.1 Particle Image Velocimetry (PIV) System

A Dantec FlowMap 1500 2D Particle Image Velocimetry (PIV) apparatus (Dantec Dynamics A/S, Tonsbakken 16 – 18, DK – 2740 Skovlunde, Denmark) was used to determine the velocity flow field and turbulence intensity inside the dissolution vessel in both testing system and standard system. The PIV system comprised a double pulsed 120 mJ Nd-Yag laser (New Wave Research model Solo 120 15 Hz, Fremont, CA, USA), a digital camera (Dantec Dynamics HiSense PIV/PLIF camera model C4742-53-12NRB) with a charge coupled device (CCD) chip, a synchronizer (LASERPULSE Synchronizer, TSI model 610034) and the software (FlowManager 4.71) installed in a computer (DELL Precision WorkStation 530), as shown in Figure 2.7.

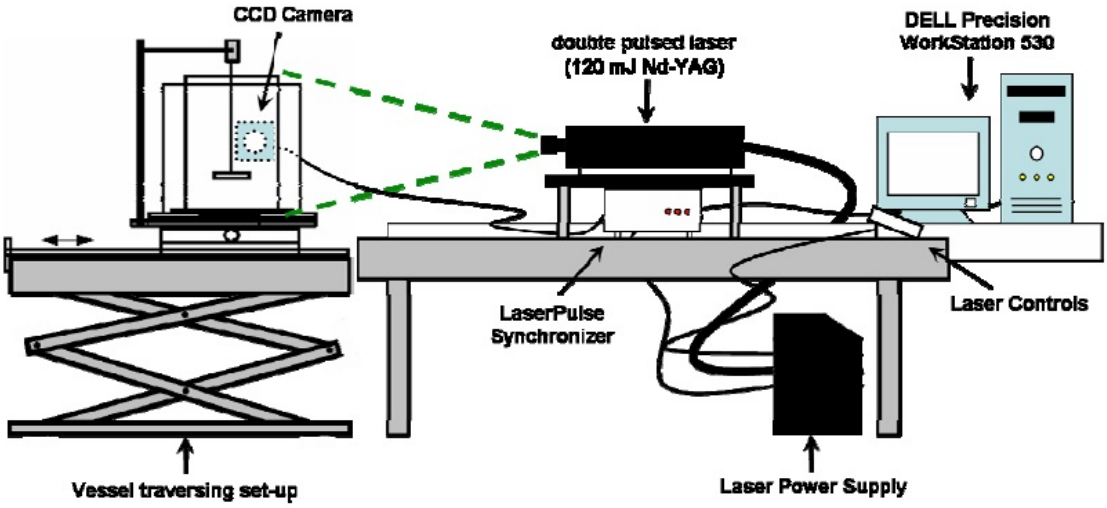

Figure 2.7 Schematic of laboratory PIV experimental set-up.

In the PIV experiment, the dissolution vessel was placed in an external Plexiglas square tank filled with water in order to minimize refractive effects at the curved surface of the vessel wall. Black plastic shaft and impeller were specially used to minimize the reflection of the laser light impinging on them. The agitation was kept 100 rpm and provided by an electric motor connected to an external controller. The water (900 mL) in the dissolution vessel was seeded with trace amounts of 10 μm silver-coated hollow borosilicate glass spheres (Dantec Measurement Technology USA, Mahwah, NJ, USA) which were used to follow the fluid flow and scatter the laser light for fluid velocity measurements.

The light source of the PIV system came from the Class IV Nd-Yag laser, consisting of two infrared laser heads combined in a single package with a second harmonic generator and two discrete power supplies and emitting 532 nm wavelengths light. Two pulsed infrared laser beams were produced by the laser and passed through an optical arrangement of lenses to generate a laser light sheet. When the laser light sheet

was shot through the dissolution vessel with seed particles in the water, the light scattered by these particles was captured by the CCD camera which was installed next to the tank at a 90º orientation with respect to the laser light sheet. A light filter is fitted in front of the camera lens to remove visible light and any incident laser light from reflection. The camera and the laser were connected to the synchronizer which was then in turn connected to the computer running the FlowManager 4.71 software for test control and data analysis. Pairs of digitized images of illuminated particles in the dissolution vessel from the camera were subdivided into small subsections called interrogation areas via the software and then were analyzed using cross-correlation to determine the spatial x- and y-displacement that maximized the cross-correlation function for that interrogation area. The resulting displacement vector obtained by dividing the x- and y- displacements by the time interval was taken as the fluid velocity in that interrogation area.

2.2.2 PIV Method

In the PIV experiment, the velocity profiles on only one-half section of the vessel could be measured due to the shaft blocking the laser light sheet. In the standard system, only one lengthwise cross-section of the vessel was studies, since the standard system (without the cannula) was symmetrical. In the system with the cannula, the velocity profiles were measured on four lengthwise cross-sections, 90° apart from each other, since this system was non-symmetrical because of the presence of the cannula in the medium. Using the tablet position numbering mentioned before (Figure 2.6 (a)), the four sections were named Section A, Section B, Section C and Section D, as shown in Figure 2.8. However, when studying Section A, the cannula could block the laser light sheet. Therefore, two additional PIV measurements were conducted in order to show the velocities on vertical

planes just before or just behind the cannula: Section A-Front was the vertical section where the laser sheet was just in front of the cannula (by about 2 mm) while Section A-Back, where the laser sheet was just behind cannula (by about 2 mm), as shown in Figure 2.8 and Figure 2.9. The PIV measurements were conducted three times for all sections, except the Section A-Front and Section A-Back.

A PIV measurement consisted of taking a pairs of images at a time interval of 1 ms. In each PIV test, 300 image pairs in total were captured by the CCD camera, at a time interval of 1000 ms between each pair. Then, image masks were defined and applied to all images to reject the impeller and shaft regions, and the obscured regions not illuminated by the laser and all external regions, in order to reduce the error in cross correlation. Each image was divided in interrogation areas 16 pixels x 16 pixels. Cross-correlation was employed on each interrogation areas in each image pair to determine the most likely velocity vector that best resulted in the first interrogation area being superimposed on the second. That velocity vector was taken to be the velocity projection of the fluid velocity on that vertical section. For each interrogation area, the final velocity vector on the vertical section was taken to be the statistical average of the 300 pairs image pairs. By applying this approach to each area the velocity profile on the entire section was obtained. The profile then went through moving-range validation and average filter to obtain the final velocity vector map for further analysis. (FlowMap PIV Installation & User's guide, 2000)

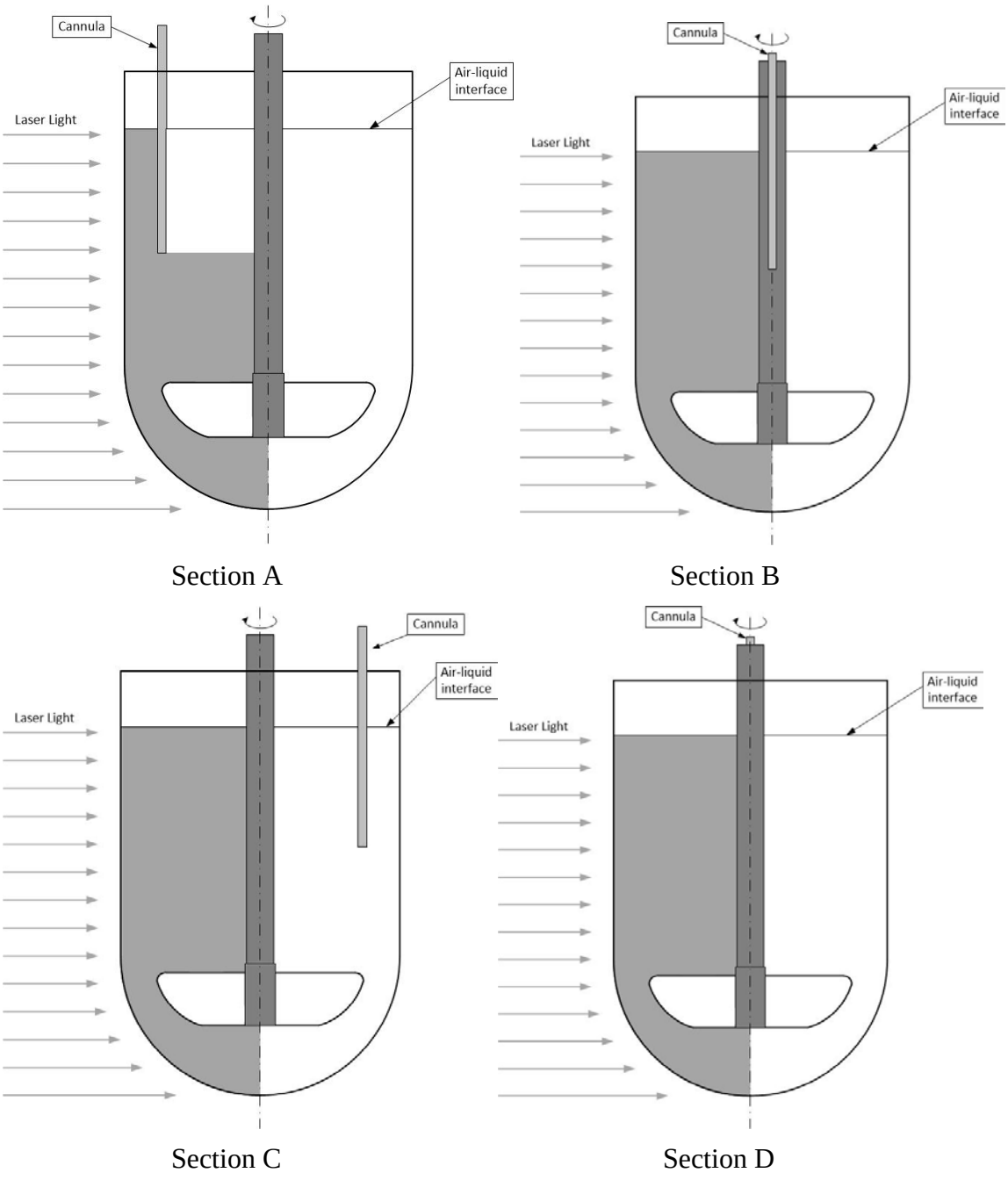

Figure 2.8 Schematic of the sections (in grey) studied using PIV.

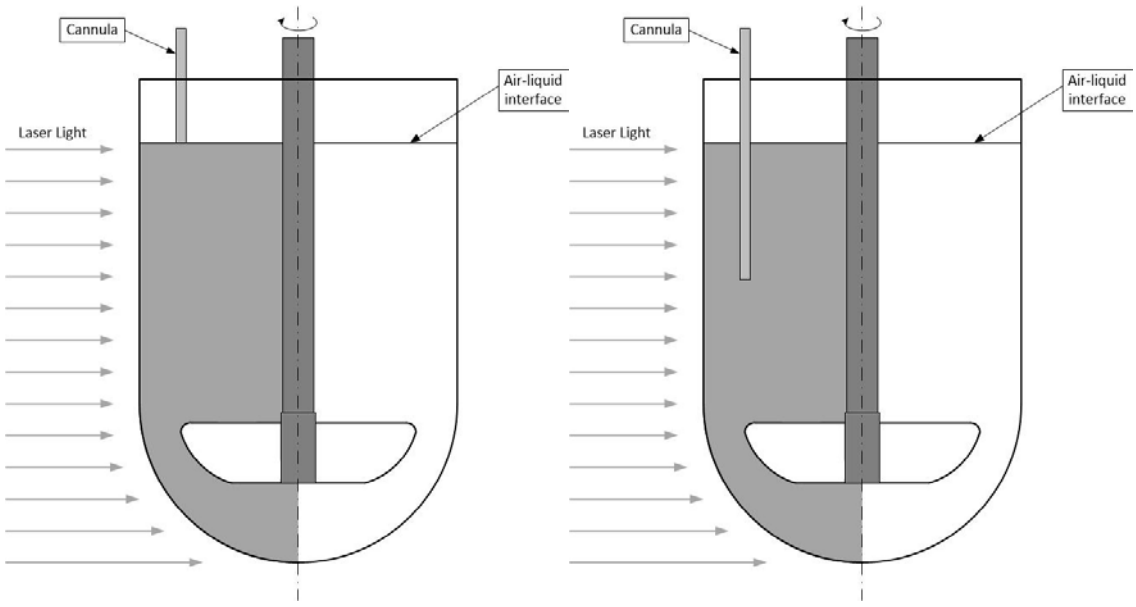

Section A-Front Section A-Back

Figure 2.8 Schematic of the sections (in grey) studied using PIV (Continued).

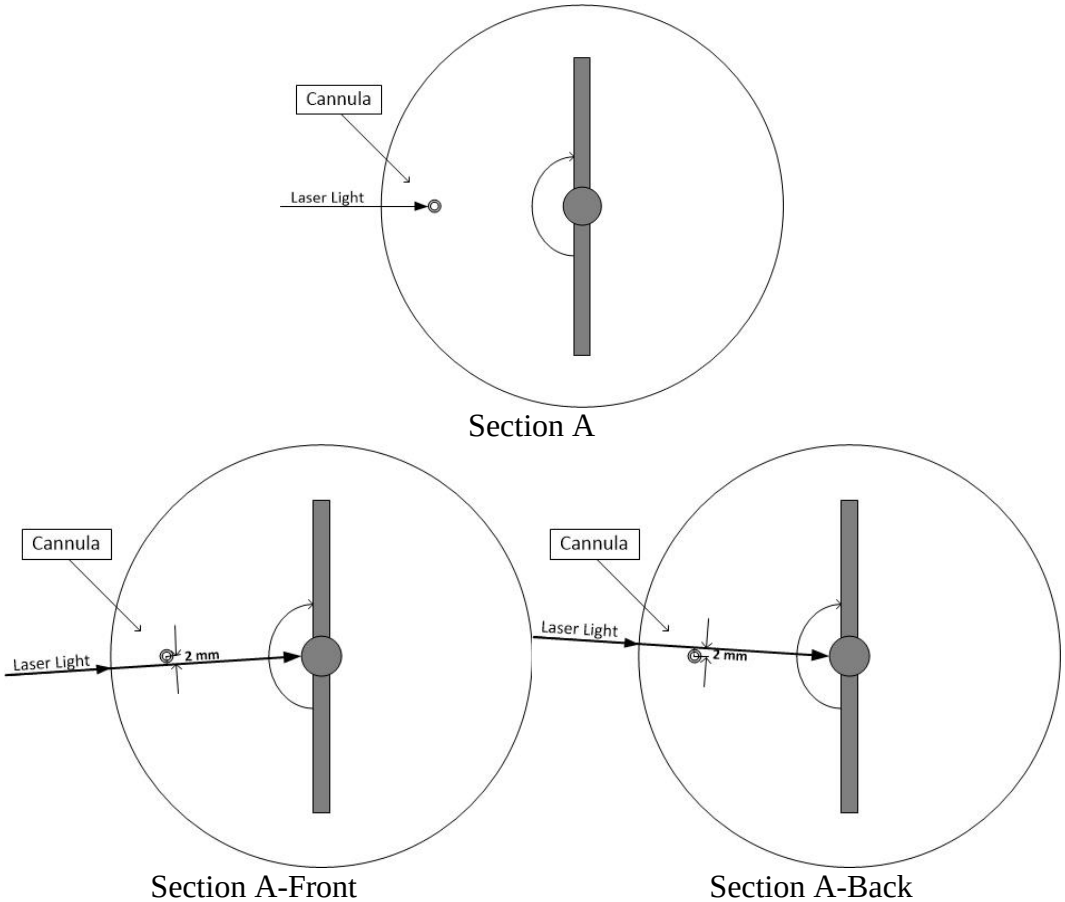

Section A

Section A-Front Section A-Back

Figure 2.9 Schematic of the top views in Section A, Section A-Front and Section A-Back.

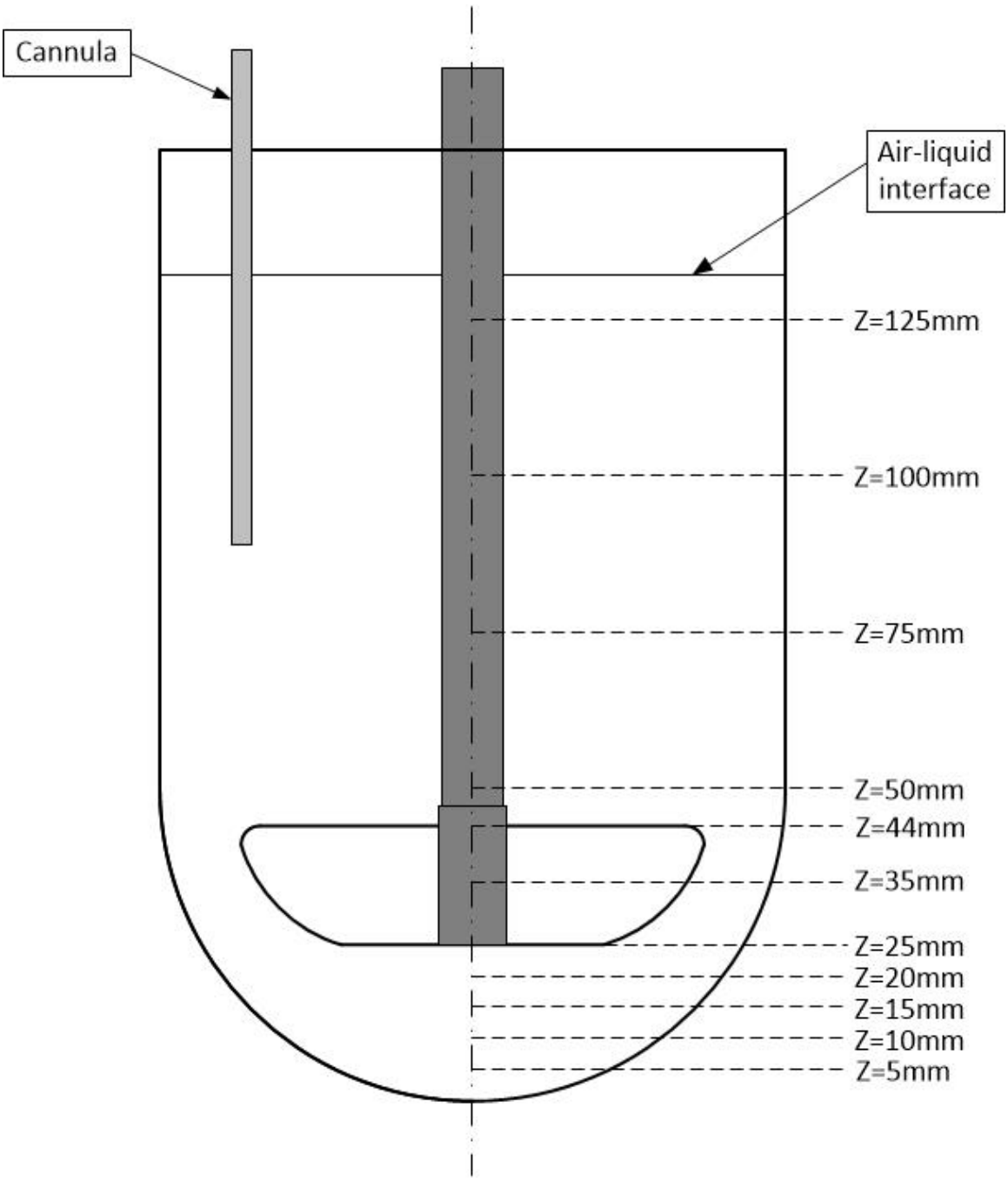

Figure 2.10 Eleven iso-surfaces chosen for PIV measurements.

The liquid velocity at any point in the vessel has three components: radial velocity, acting in a direction perpendicular to the shaft of the impeller; axial velocity, acting in a direction parallel with the shaft; and tangential velocity, acting in a direction

tangent to a circular path around the shaft. In this 2-D PIV study, only the axial and radial velocities were investigated.

To fully quantify the fluid flow in the dissolution vessel, eleven iso-surfaces at different vertical (z) positions were selected along the height of the vessel, as shown in Figure 2.10. The bottom of the vessel was taken as the iso-surface at z = 0 mm. Four iso-surfaces were chosen below the impeller (z = 5 mm, 10 mm, 15 mm and 20 mm). Three were chosen in the impeller region: the bottom edge of the impeller, i.e., z = 25mm, the middle of the impeller, i.e., z = 35mm, and the top edge of the impeller, i.e., z = 44mm. Four were chosen above the impeller: z = 50 mm, z = 75 mm, z = 100 mm and z = 125 mm. The average radial and axial velocities and standard deviation for each data point on each iso-surface were extracted, plotted and analyzed.

In order to determine the reproducibility of the PIV measurement and to determine the suitability of the instrument to detect differences between velocities in the standard system and in the testing system, six identical experiments with the standard system alone were conducted. The average standard deviations in those three regions, i.e., below the impeller, around the impeller and above the impeller, were calculated and presented.

Sums of squared deviations were calculated to compare the velocity profiles on the four sections of the testing system to those of the standard system.

$$S = \sum \frac{(U - U_0)^2}{{U_{tip}}^2} \tag{2.7}$$

where U is the velocity of the testing system and U_0 is the corresponding velocity of the standard system at the same point. By summing up all squared deviations in each of the three regions, i.e., below the impeller, around the impeller and above the impeller, as well as in the whole section, the hydrodynamic effect generated by the cannula could be identified and quantified.

CHAPTER 3

RESULTS

As mentioned in Chapter 2, the objective of this project was to quantify the hydrodynamic effects introduced by the presence of a cannula in a USP Dissolution Testing Apparatus 2 by the dissolution test and PIV measurement. The dissolution profiles obtained in the two systems (standard system and testing system) were compared by plotting m_D/m_T (fractional drug release) against time (min) and evaluating the difference using statistical tools. The velocity profiles obtained from the PIV measurements for the two systems were also compared by visualizing the flow velocity vectors and quantitatively analyzing the velocities on eleven iso-surfaces.

3.1 Results of the Dissolution Tests

In order to determine the effect of the cannula in dissolution tests, experimental data obtained from two systems, with and without cannula, were examined for all nine different tablet positions. The averages of triplicate experimental dissolution profiles at each tablet position are presented in terms of m_D/m_T against time together with the standard deviations of three replicates (Figure 3.2 through Figure 3.10). The results of the dissolution test following the USP procedure is shown in Figure 3.11. The difference factor (f_1), similarity factor (f_2) and probability associated with the Students' t-test (P(t-test)) were calculated for the averages of triplicate experimental profiles at each tablet position, and are presented in Table 3.2.

3.1.1 Calibration Results for Salicylic Acid Tablets

Calibration was performed following the method described in Section 2.1.3. A series of salicylic acid solution with known concentration were detected by the UV spectrophotometer at the wavelength 296 nm. This process was initially performed twice to establish the conversion from UV absorbance to salicylic acid concentration, and repeated every 3 months, without showing significant change. The results are presented in Table 3.1 and Figure 3.1 for two sets of calibration experiments.

Table 3.1 Calibration Data for Prednisone Tablets

Concentration (mg/ml)	**Absorbance 1**	**Absorbance 2**	**Average Absorbance**
0.00000	0.036	0.036	0.036
0.00234	0.090	0.092	0.091
0.00469	0.145	0.145	0.145
0.00938	0.252	0.253	0.2525
0.01875	0.467	0.470	0.4685
0.03750	0.895	0.899	0.897
0.07500	1.711	1.717	1.714

The difference between the two set of absorbance data was minor, and the R^2 value of the regression was 0.9998. Therefore, a linear relation between UV absorbance and concentration was confirmed in this concentration range (0 – 0.075 mg/mL). The equation displayed in Figure 3.1 was used to obtain the sample concentration from absorbance data.

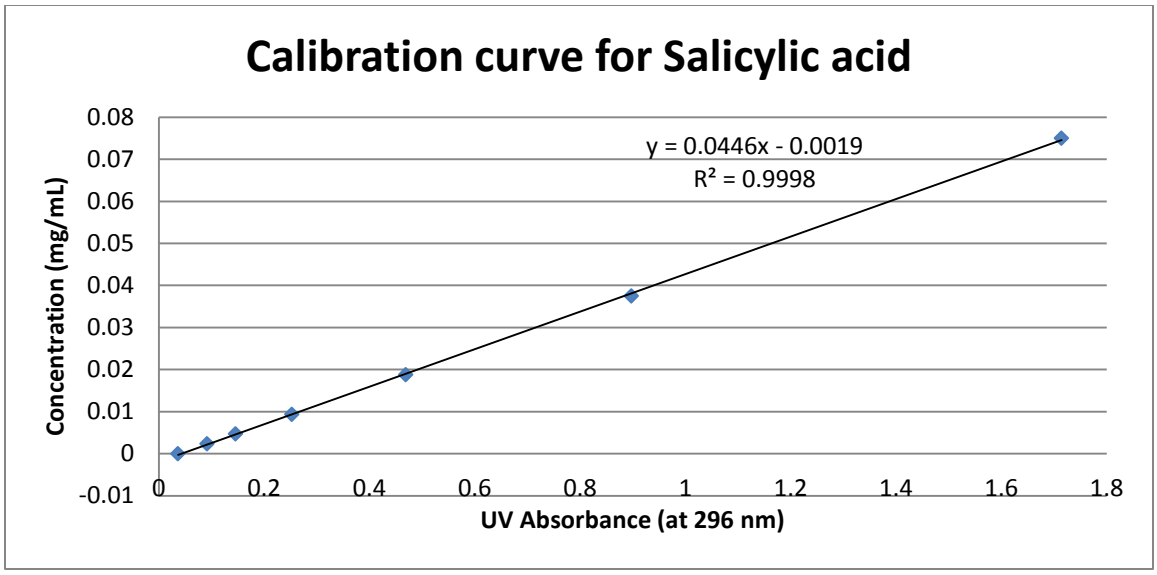

Figure 3.1 Calibration curve and regression for Salicylic Acid tablets.

3.1.2 Dissolution Profiles for Centered Tablets (Position O)

The dissolution profiles for the tablets in the center position are presented in Figure 3.2. This figure shows that the difference between the dissolution profiles for the testing system (with cannula) and the standard system (without cannula) is that at all times the average mass percentage of drug dissolved in the testing system was higher than in the standard system. Each individual paired experiment replicate also showed this difference (results are not shown here). The average standard deviations for the drug release mass ratios (m_D/m_T) in Figure 3.2 were 1.08% and 1.54% for the dissolution profiles with and without cannula, respectively. The value of paired Student's t-test, i.e., the probability that the dissolution profiles came from the same population, was 0.000209 (Table 3.2), which was much lower than the significance level of 0.05. On the other hand, the values of f_1 factor and f_2 factor, quantifying the significance of similarity/difference of two dissolution profiles, were 12.25, 86.17, respectively, which were both within the FDA

required range ($0<f_1<15$ and $50<f_2<100$). Although the value of f_1 factor (12.25) was not too distant from the upper limit f_1 (15), those values were considered to be acceptable.

Table 3.2. Average Values of P(t-test), f_1 and f_2 for Dissolution Tests at Each Tablet Position

Tablet Position		**P (t-test)**	f_1	f_2
Centered	O	0.000209	12.25	86.17
10° off-center	A1	0.000290	17.14	74.81
	B1	0.001038	3.03	96.93
	C1	0.000129	12.03	83.42
	D1	0.005908	4.37	92.97
20° off-center	A2	0.000313	6.81	88.72
	B2	0.002889	1.64	98.55
	C2	0.000042	1.42	99.16
	D2	0.021561	2.84	94.69
Dropped Tablets (USP Procedure)		0.000082	6.87	90.89

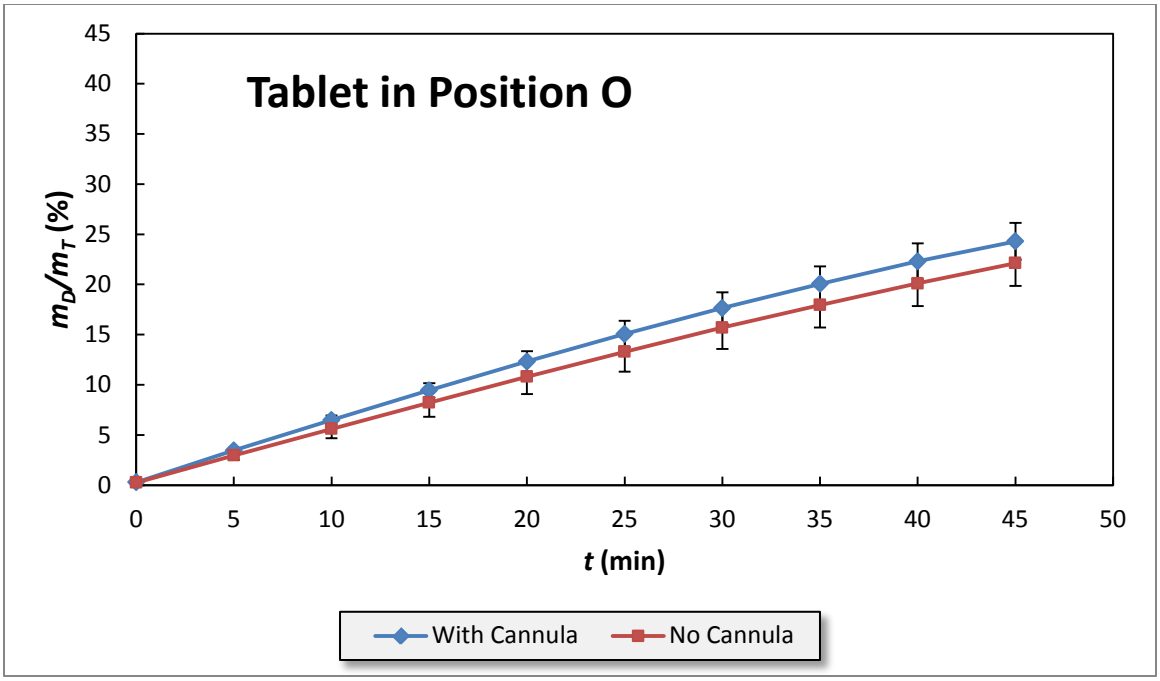

Figure 3.2 Dissolution profiles for experiments with tablets in Position O in the presence and absence of the cannula.

3.1.3 Dissolution Profiles for 10° Off-Center Tablets (Positions A1, B1, C1, and D1)

The results for the tablet on the 10° off-center circle positions are shown in Figure 3.3 through Figure 3.6, respectively, and the corresponding statistics are presented in Table 3.2. The average standard deviations for the drug release mass ratios (m_D/m_T) on the 10° circle positions were 1.12% and 1.44% for the dissolution profiles in the two systems with and without cannula, respectively. The values of Student's t-test were all much lower than the significant level 0.05 for all 10° off-center tablet positions.

Compared to the dissolution profiles for tablets in the center of the vessel bottom (Position O), the drug release fractions (m_D/m_T) for tablets on this circle were always much higher. For example, at t = 45 min, m_D/m_T was typically about 27-33% for the 10° off-center tablets whereas it was only about 22-24% for the centered tablets. These results were in agreement with previously reported work (Wang and Armenante, 2012).

For all the four positions on 10° off-center circle, the tablets in the system with the cannula generated higher dissolution profiles than those in the standard system without cannula. However, the intensities of the differences between the profiles from two systems were different depending on the tablet locations. The tablet position that produced the most different dissolution profiles on 10° circle was Position A1, which was the closest to the cannula. The calculation of difference factor f_1, similarity factor f_2 and Student's t-test confirmed this observation: f_1 had the largest value of all tablets positions (17.14), f_2 the smallest (74.81) and P(t-test) value was much less 0.05. In fact, Position A1 was the only case for which $f_1>15$, resulting in a test failure.

The next most significant difference between profiles was at Position C1. Tablets in Position B1 and Position D1 were much lesser affected by the presence of the cannula, as indicated by the smaller value for f_1 (3.03, 4.37) and larger value for f_2 (96.93, 92.97) for this case compared to other tablet positions (Table 3.2). However, the Student's t-test value was still very small (0.001038, 0.005908) for Position B1 and Position D1, indicating that the two curves were still statistically different (P(t-test)<0.05).

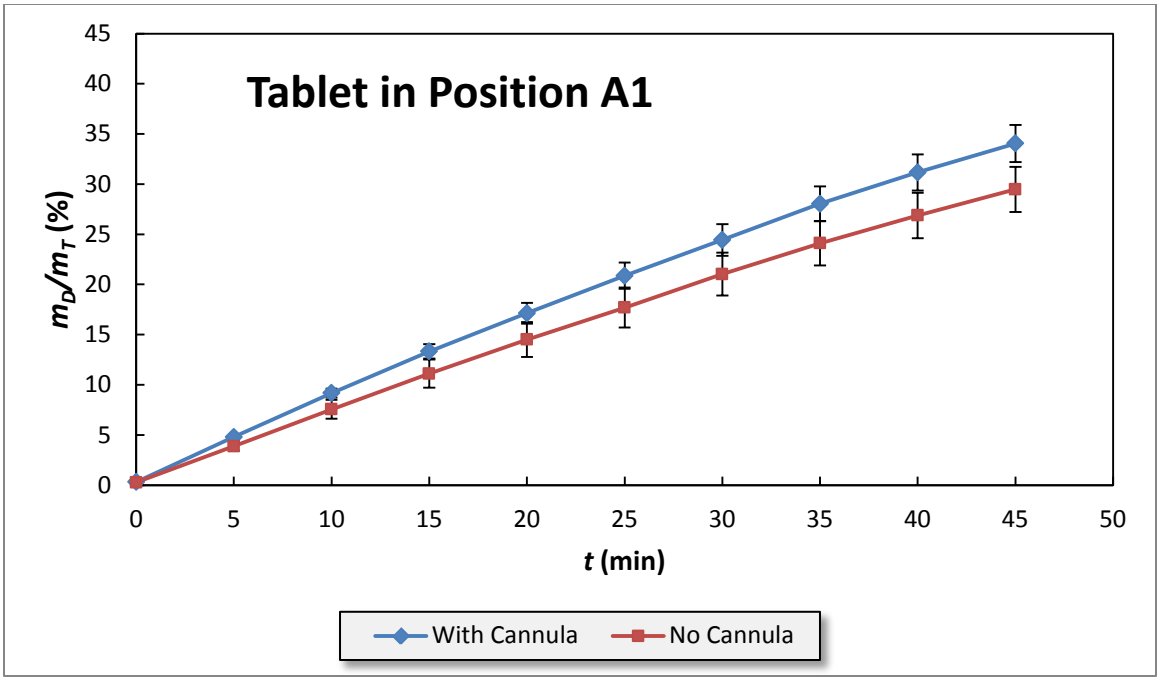

Figure 3.3 Dissolution profiles for experiments with tablets in Position A1 in the presence and absence of the cannula.

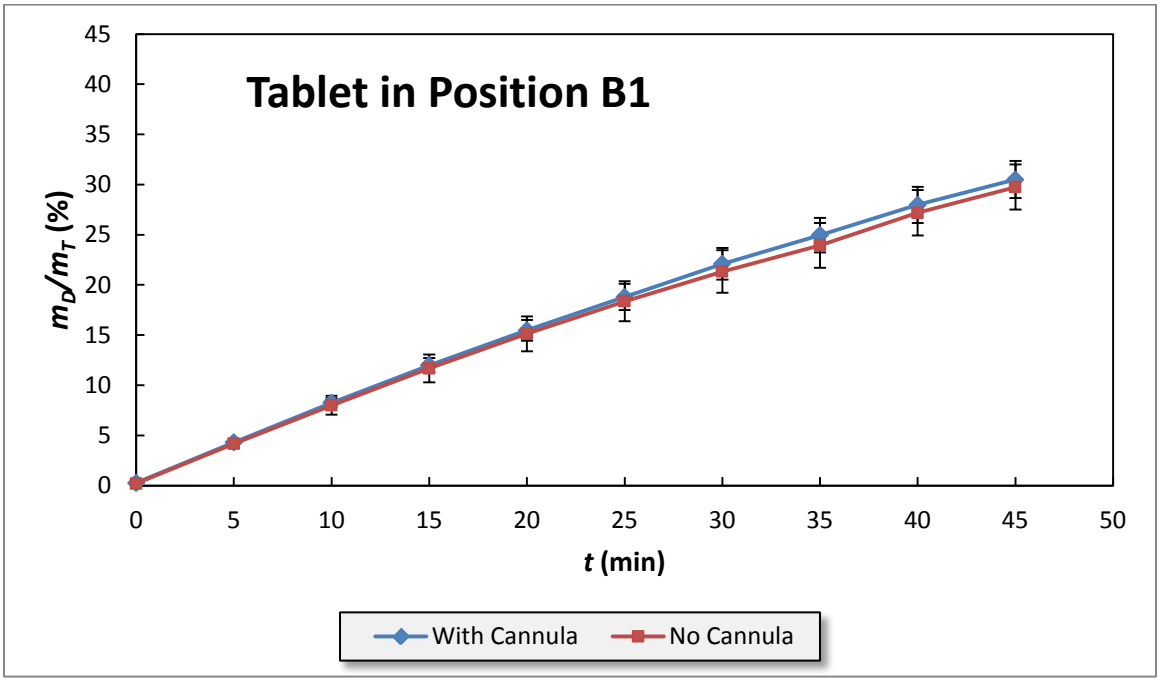

Figure 3.4 Dissolution profiles for experiments with tablets in Position C1 in the presence and absence of the cannula.

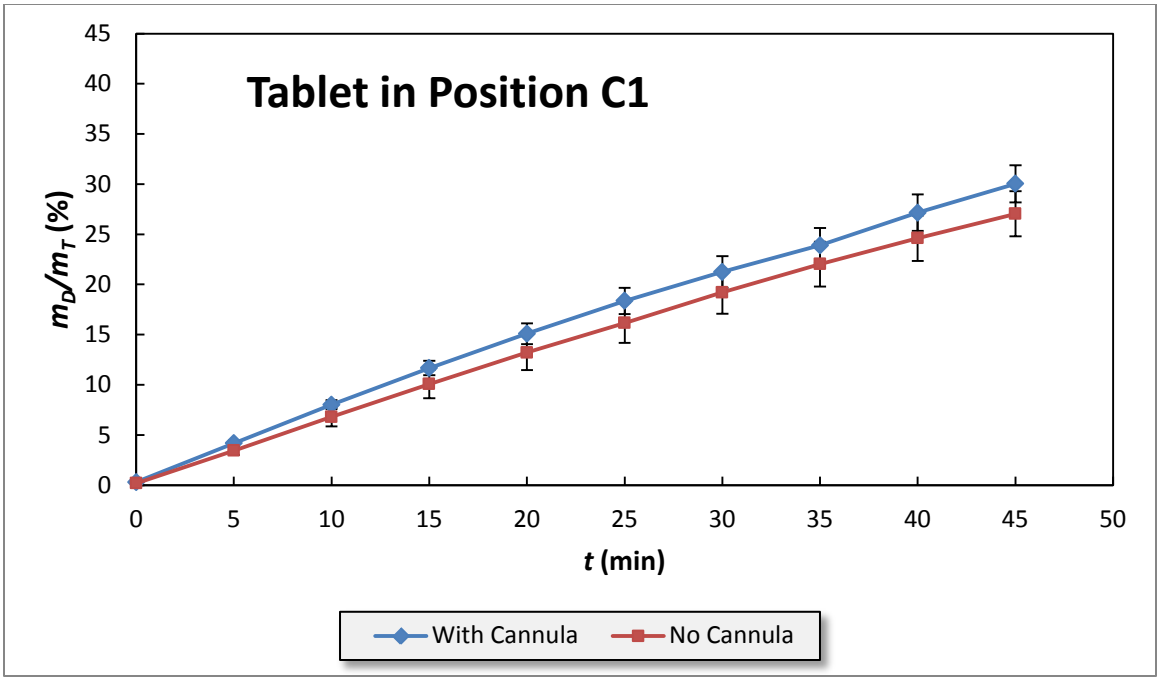

Figure 3.5 Dissolution profiles for experiments with tablets in Position D1 in the presence and absence of the cannula.

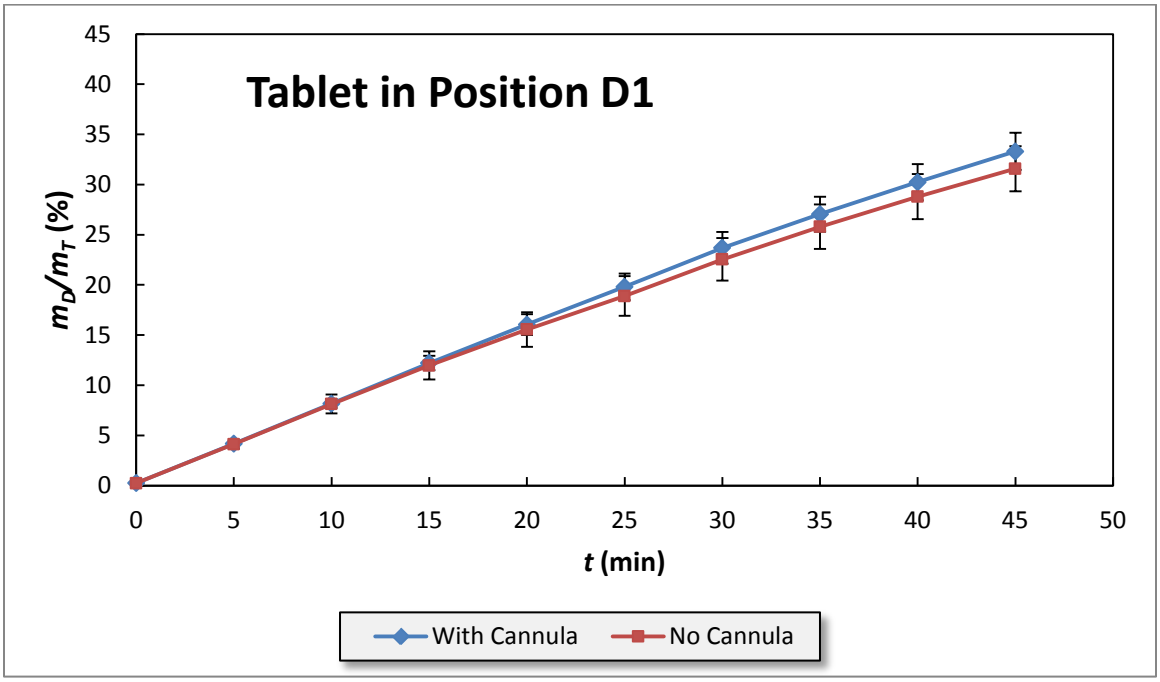

Figure 3.6 Dissolution profiles for experiments with tablets in Position B1 in the presence and absence of the cannula.

3.1.4 Dissolution Profiles for 20° Off-Center Tablets (Positions A2, B2, C2, and D2)

The results for the tablet on the 20° off-center circle positions are presented in Figure 3.7 through Figure 3.10 and the corresponding statistics are shown in Table 3.2. The average standard deviations for drug release mass ratios (m_D/m_T) in these figures were 1.26% and 1.27% for the dissolution profiles of the two systems with and without cannula, respectively. The differences between the profiles for the systems on the 20° off-center circle were less evident. In Position B2, Position C2 and Position D2 the m_D/m_T profiles for the testing system were nearly identical or even below those for the standard system. However, their values of t-test were still lower than the significance level of 0.05, indicating that the two profiles were still statistically different. Only for Position A2 the difference between the dissolution profiles for the two systems, was noticeable, although only to a limited extent. For all positions in the 20° off-center circle, the f_1 and f_2 values were in the appropriate range to pass the dissolution test, even for the Position A2 (f_1 =6.81, f_2 =88.72).

The dissolution profiles of tablets on the outer circle (20° off-center circle) were always higher comparing to those on the inner circle (10° off-center circle), as previously reported (Wang and Armenante, 2012). The results for tablets on two circles show some similarities. Tablets nearest to the cannula (Positions A1 and A2) produced higher differences between dissolution profiles with and without the cannula. However, in all cases, the effect of the cannula was more pronounced when the tablets were on the inner circle than when they were on the outer circle.

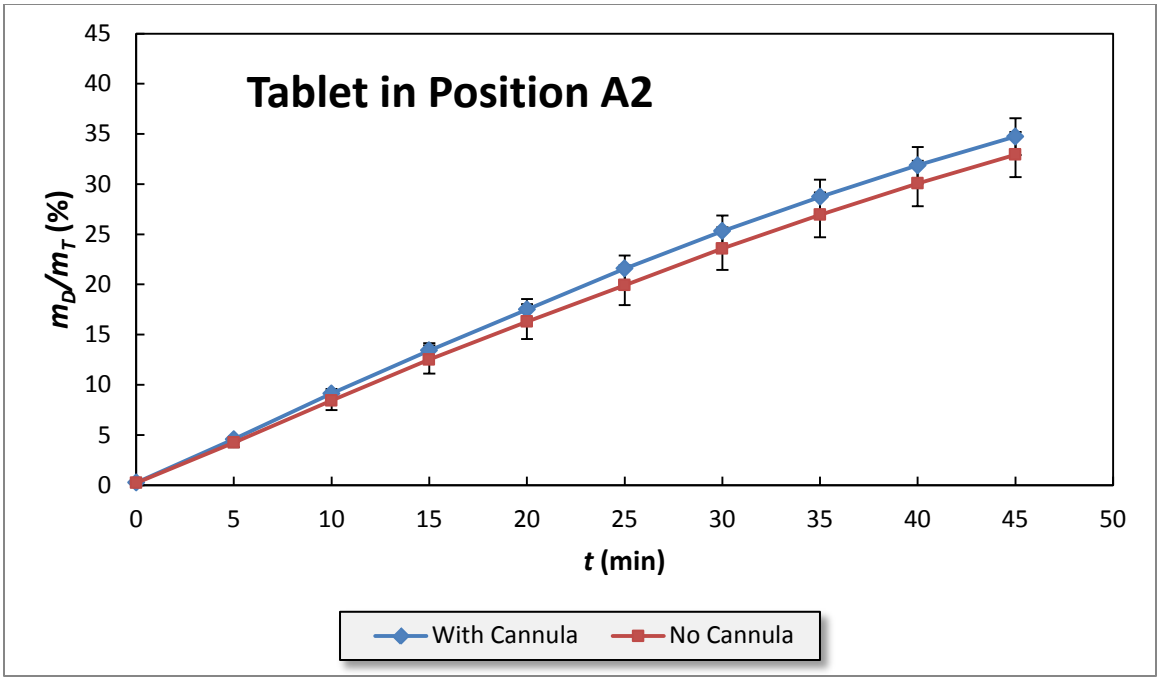

Figure 3.7 Dissolution profiles for experiments with tablets in Position A2 in the presence and absence of the cannula.

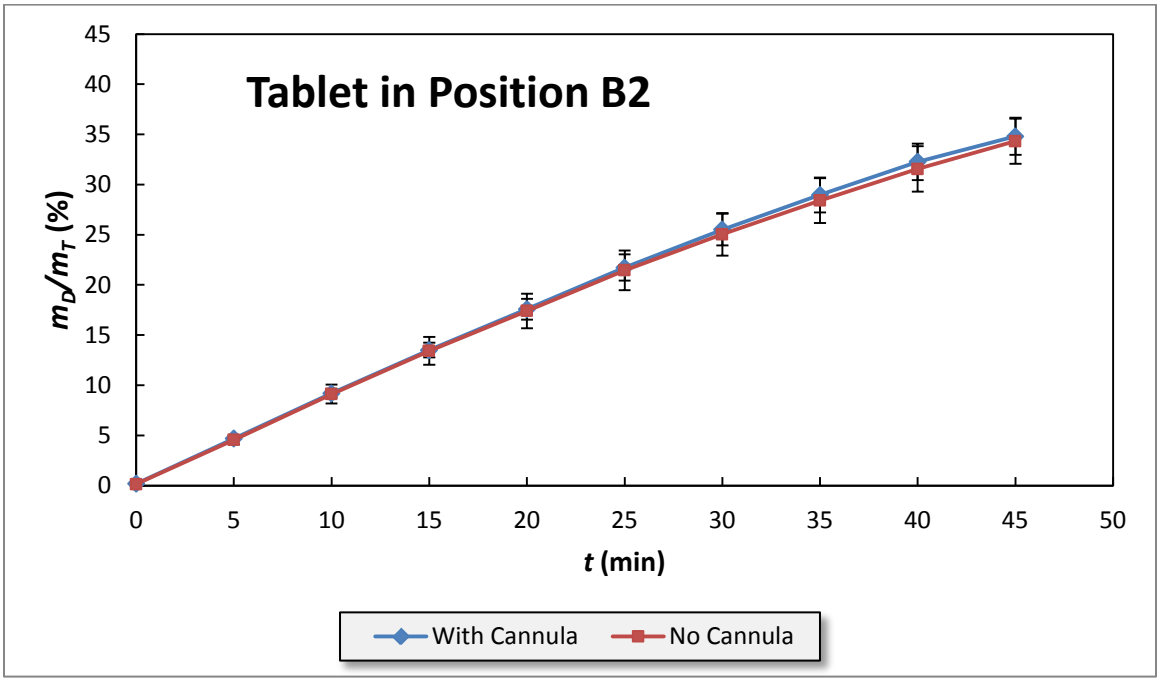

Figure 3.8 Dissolution profiles for experiments with tablets in Position B2 in the presence and absence of the cannula.

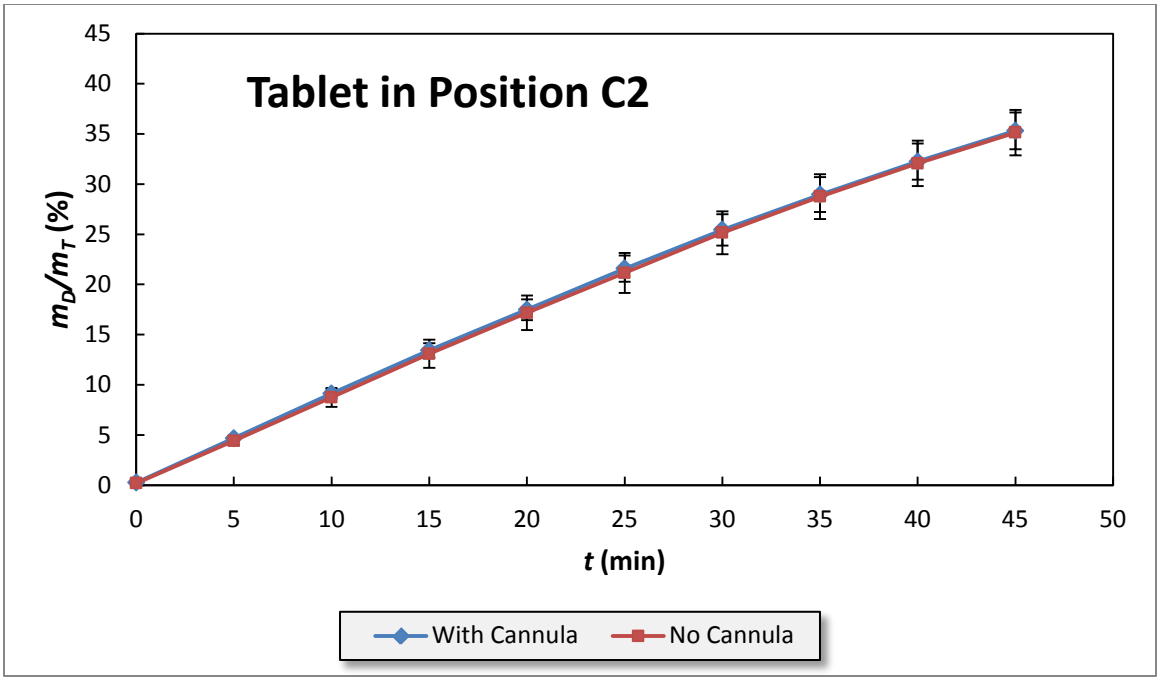

Figure 3.9 Dissolution profiles for experiments with tablets in Position C2 in the presence and absence of the cannula.

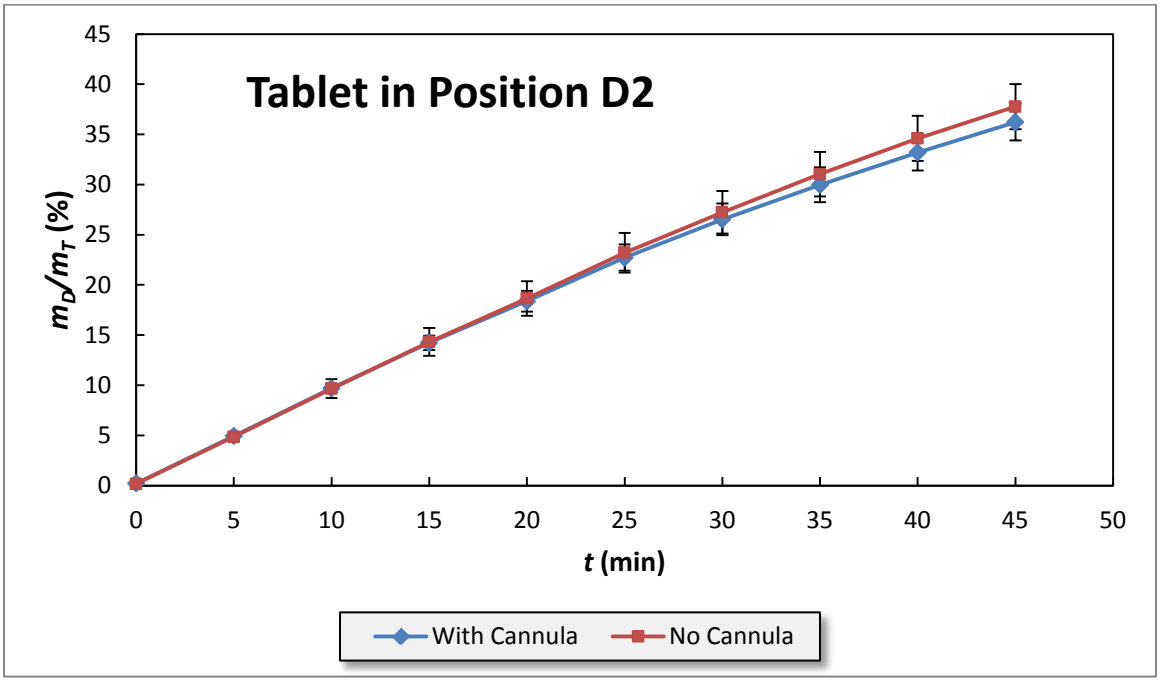

Figure 3.10 Dissolution profiles for experiments with tablets in Position D2 in the presence and absence of the cannula.

3.1.5 Dissolution Profiles for the Tablets using USP Dissolution Procedure

According to the USP (2012), in the standard dissolution test the tablet is dropped into the vessel after the medium had been added to the vessel and heated to 37ºC. The results for the tablets using the USP dissolution procedure are shown in Figure 3.11, and the corresponding statistics are shown in Table 3.2. The average standard deviations for the drug release mass ratios (m_D/m_T) were 0.36% and 1.04% for dissolution profiles in the standard system and the testing system, respectively. The dissolution profile obtained from the testing system was slightly higher than that obtained from the standard system. The value of the Student's t-test (0.0000816) was much smaller than the significance level (0.05). The values of f_1 and f_2 factors were 6.87, 90.89 respectively, which were both within the FDA required range ($0< f_1 <15$ and $50 < f_2 <100$).

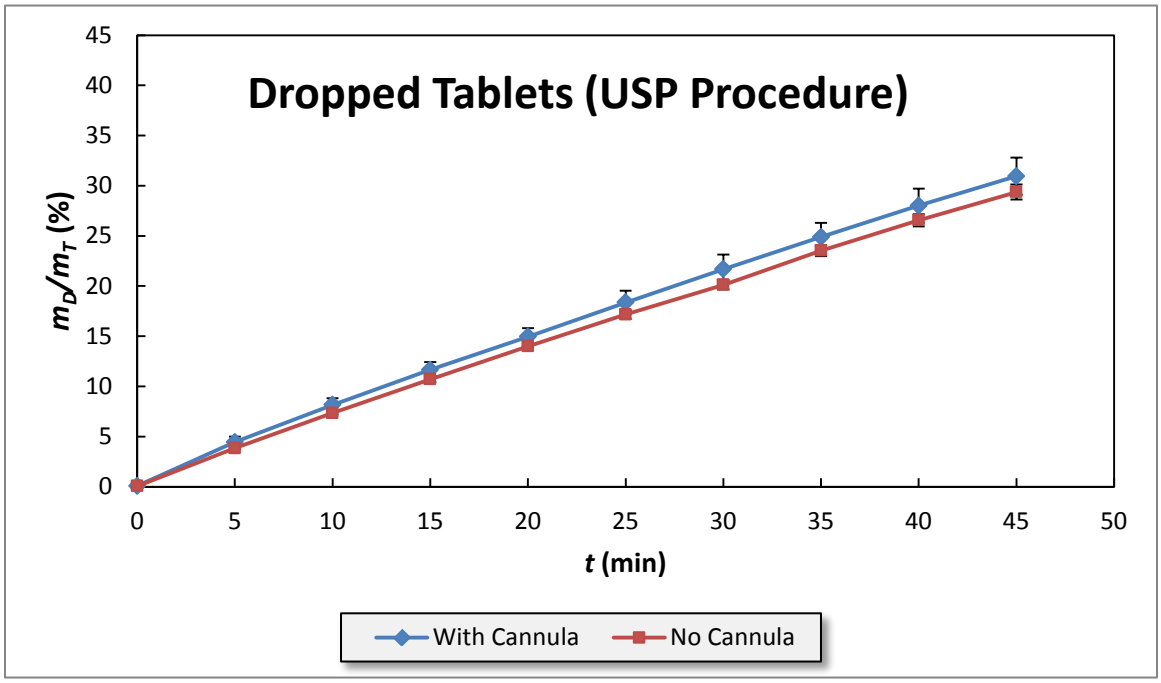

Figure 3.11 Dissolution profiles for experiments with tablets using USP Procedure in the presence and absence of the cannula.

3.2 Results of PIV Measurement

3.2.1 Velocity Vectors

The velocity vectors maps of the two systems are shown in Figure 3.12 and Figure 3.13. In order to shown the entire velocities vector in Section A, two other tests (Section A-Front, i.e., the laser sheet was in front of the cannula, and Section A-Back, i.e., the laser was behind the cannula) were conducted and also presented in Figure 3.13. The vectors in each of the images were scaled according to their magnitudes using the same scale factor. The vectors were color-coded in order of increasing velocity magnitude. The vectors with the lowest velocities were plotted in dark blue, followed by light blue, green, yellow, orange and red, which represented the highest velocities.

The overall flow patterns that emerged from the vector maps were found to be similar, as shown in Figure 3.12 and Figure 3.13. A big but weak recirculation loop dominated by the axial velocity component generated by the impeller rotation can be observed in the upper region of the vessel. Near the vessel wall (R/R_0> ~0.7) this flow was directed upwards, while in the middle inner core region above the impeller (~0.3 < R/R_0< ~0.7), the flow was directed downwards. In the innermost core region (R/R_0< ~0.3), the flow is characterized by very low axial and radial velocities. The fluid region around the impeller was dominated by the impeller rotation (Bai et al., 2007). The axial and radial velocities changed significantly in this region. The flow in the region below the impeller is the most important and complex for this work. All test sections show that the flow in this region was very weak, especially the inner region just below the shaft at the center of the vessel bottom. In this region, there was another recirculation loop formed by the downwards flow produced by the agitation of the impeller and the vessel

wall. This vertical recirculation loop was not able to penetrate the weak inner core region. The flow patterns in the standard system are in agreement with those obtained in previous studies (Bai et. al., 2007, Bai et al., 2009).

Despite the similarity between figures, two major differences could be observed. Firstly, in almost all sections in the system with the cannula the recirculation loop above the impeller became more intense, especially in the middle inner core region. The most significant effect was on Section A (Back), followed by Section B and Section C, and this effect seemed to disappear in Section D. This makes intuitive sense, in that the intensity of the disturbances introduced by the cannula extends downstream of the cannula but with decreasing intensity. Secondly, the velocities below the shaft, which is the most important region in the vessel since this is where the tablets usually stay in practice, were slightly stronger in Section A, Section A-Front and Section A-Back than in any other sections, where larger radial velocities could be found especially near the center of the vessel bottom. By contrast, in Section B, Section C and Section D, the velocities remained nearly the same as those in the standard system, or even slightly smaller.

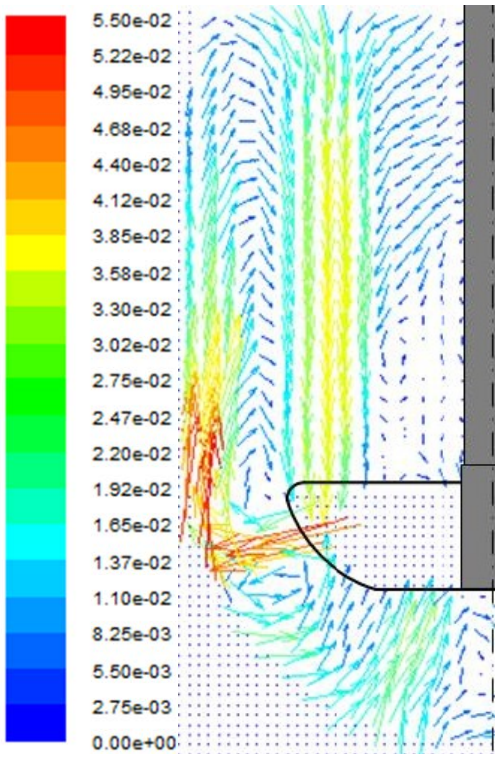

Figure 3.12 PIV velocity vectors map for the standard system (velocities are in m/s).

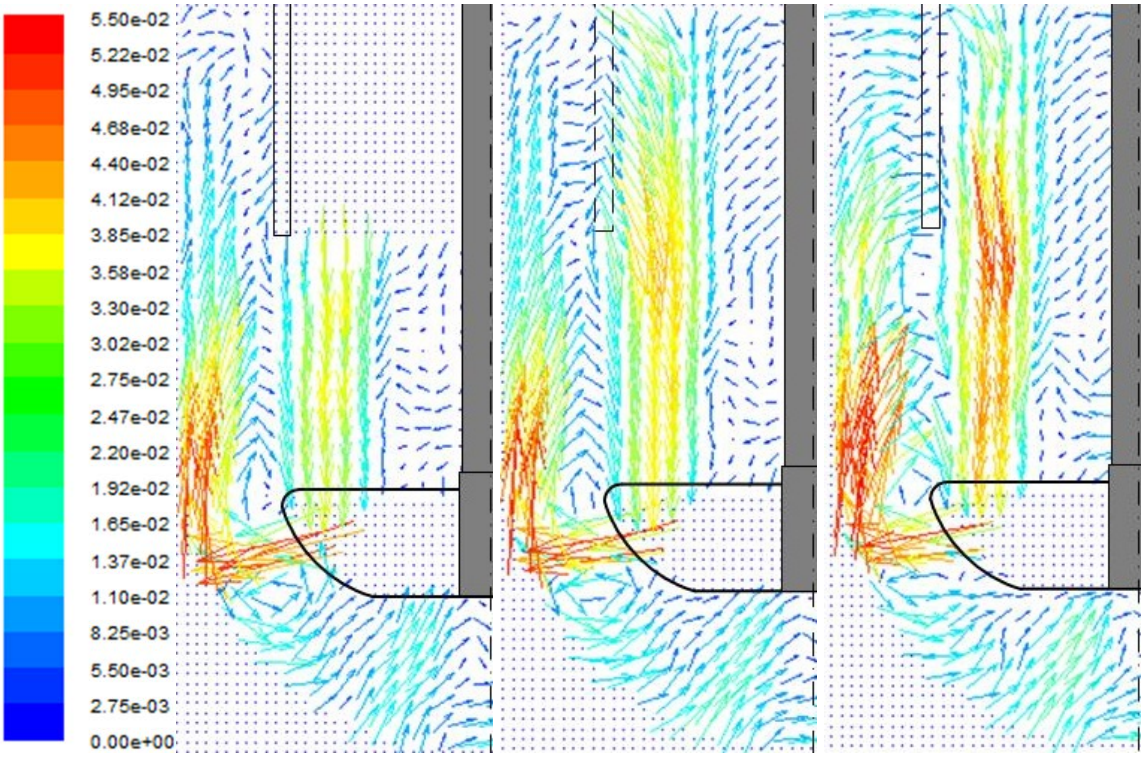

Section A Section A-Front Section A-Back

Figure 3.13 PIV velocity vectors maps for all four sections in the testing system with cannula (velocities are in m/s).

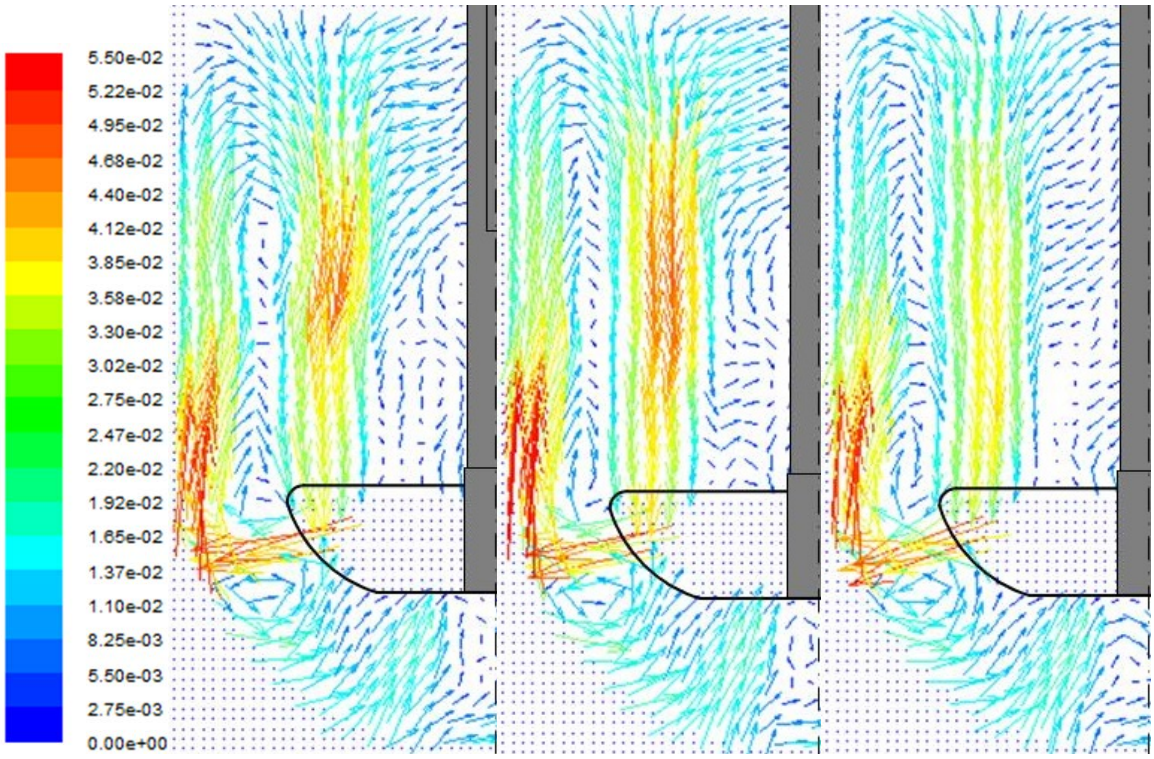

Figure 3.13 PIV velocity vectors maps for all four sections in the testing system with cannula (velocities are in m/s) (Continued).

3.2.2 Velocity Profiles on Iso-Surfaces

Figures 3.14 through 3.19 show, respectively, the radial and axial velocity profiles on eleven iso-surfaces. In these figures, the ordinates represent the normalized fluid velocity U/U_{tip} (scaled by the impeller tip speed, U_{tip}=0.388 m/s) and the abscissas represent the normalized radial position R/R_0 (scaled using the vessel radius, R_0=50.08 mm). The centrifugal radial velocity and the upwards axial velocity were defined as positive velocities. It should be remarked that the scales in these figures are different.

3.2.2.1 Reproducibility of PIV Measurements. The average standard deviations in the three regions examined here, i.e., below the impeller, around the impeller and above the impeller, are presented in Table 3.3. The PIV measurements were found to be very

reproducible in the regions below and above the impeller, while a slightly larger standard deviation was found for the velocities around the impeller, because the velocities in this region were affected by the presence of the impeller. Therefore, these velocities were larger and more turbulent, causing more variability in the velocity data.

Table 3.3 Average Standard Deviations of PIV Measurements in Three Regions for the Standard System

Region	Iso-Surfaces	Average Standard Deviation
Below the Impeller	Z=5 mm, 10 mm, 15 mm, 20 mm	0.003890
Around the Impeller	Z=44 mm, 35 mm, 25 mm	0.006907
Above the Impeller	Z=50 mm, 75 mm, 100 mm, 125 mm	0.003111
Overall Average		0.004429

3.2.2.2 Velocity Profiles below the Impeller. Figure 3.14 and 3.15 show, respectively, the average radial and axial velocity profiles and the standard deviation for each data point on iso-surfaces below the impeller, i.e., Z=5 mm, 10 mm, 15 mm and 20 mm.

In general, the differences between the velocities in this region were small in absolute value. The largest differences in radial velocities were found in the weak velocity zone blow the shaft, i.e., $R/R_0 < 0.2$ for all four iso-surfaces. The most significant velocity differences were found in Section A. Slightly higher axial velocities in Section A were also observed in a smaller zone below the shaft, i.e., $R/R_0 < 0.1$ for all four iso-surfaces. This is consistent with velocity vector maps in Section 3.2.1.

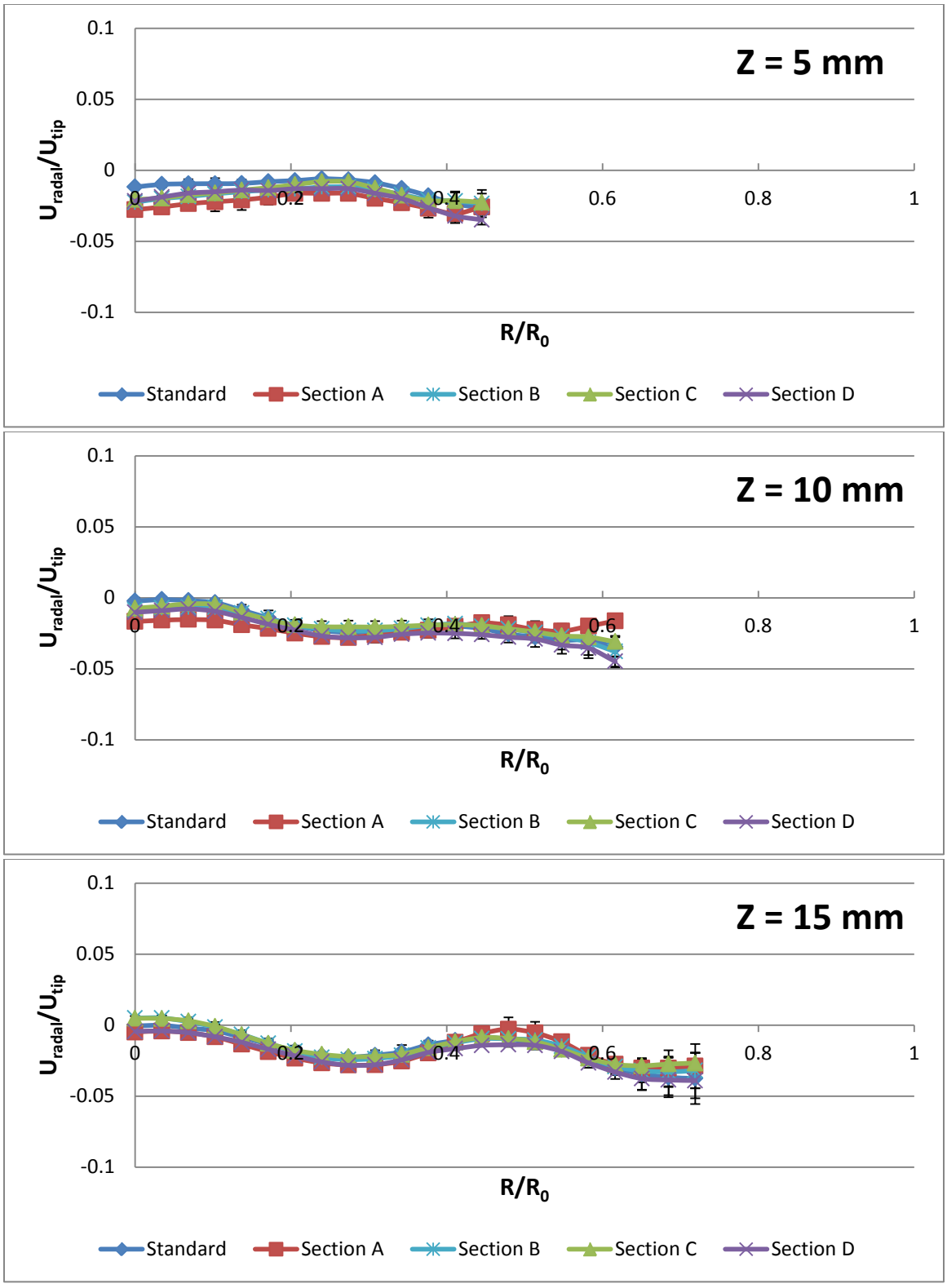

Figure 3.14 PIV measurements for radial velocities on different iso-surfaces below the impeller.

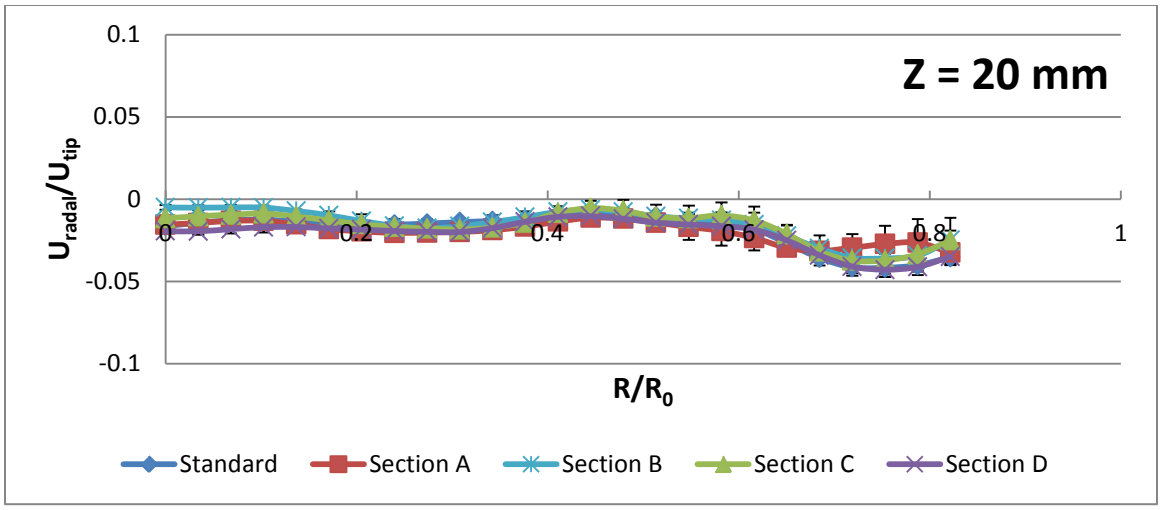

Figure 3.14 PIV measurements for radial velocities on different iso-surfaces below the impeller (Continued).

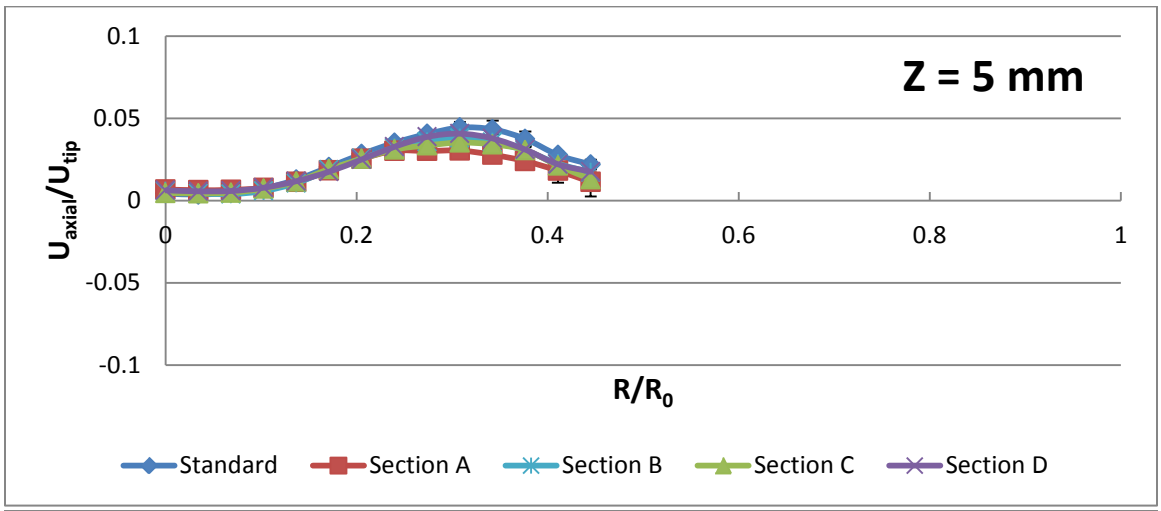

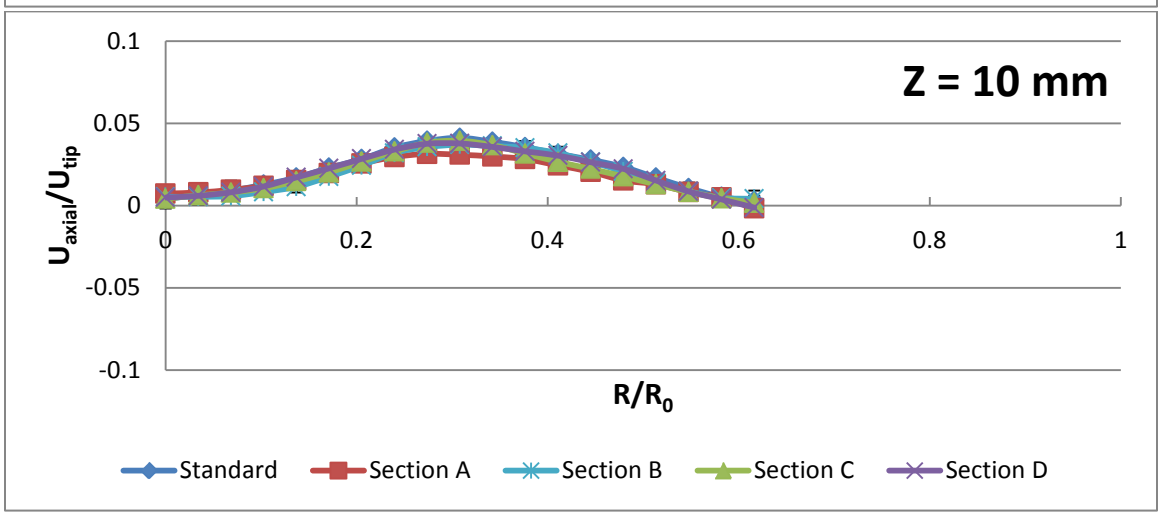

Figure 3.15 PIV measurements for axial velocities on different iso-surfaces below the impeller.

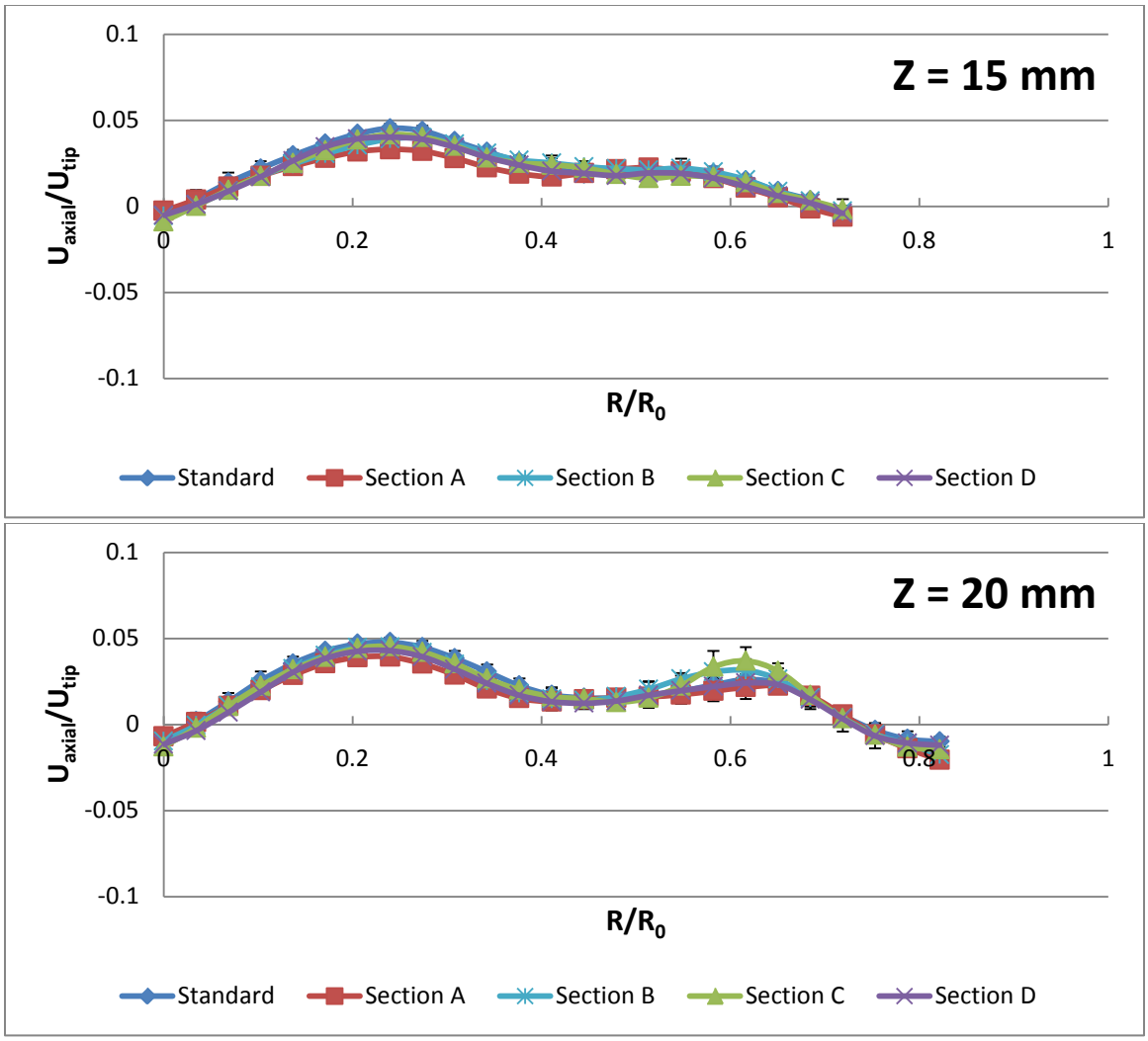

Figure 3.15 PIV measurements for axial velocities on different iso-surfaces below the impeller (Continued).

3.2.2.3 Velocity Profiles around the Impeller. Figure 3.16 and 3.17 show, respectively, the average radial and axial velocity profiles and standard deviation for each data point on the iso-surfaces around the impeller, i.e., Z=25 mm, 35 mm and 44 mm.

As shown in these figures, a larger average standard deviation in this region was obtained, which was agreement with the results of reproducibility for standard system in this region (Table 3.3). Although the differences between each section were found much larger, most data points were within the error range indicated by the error bars. However,

several differences cannot be attributed to experimental error. On iso-surface Z=35 mm, where the transition between two recirculation loop occurred, all sections showed different flow velocities compared to the standard system, indicating that the flows were stronger in this zone. On iso-surface Z=44 mm, the radial velocity in Section A was much higher than for other sections in the zone near the impeller (~0.7<R/R_0<~ 0.8).

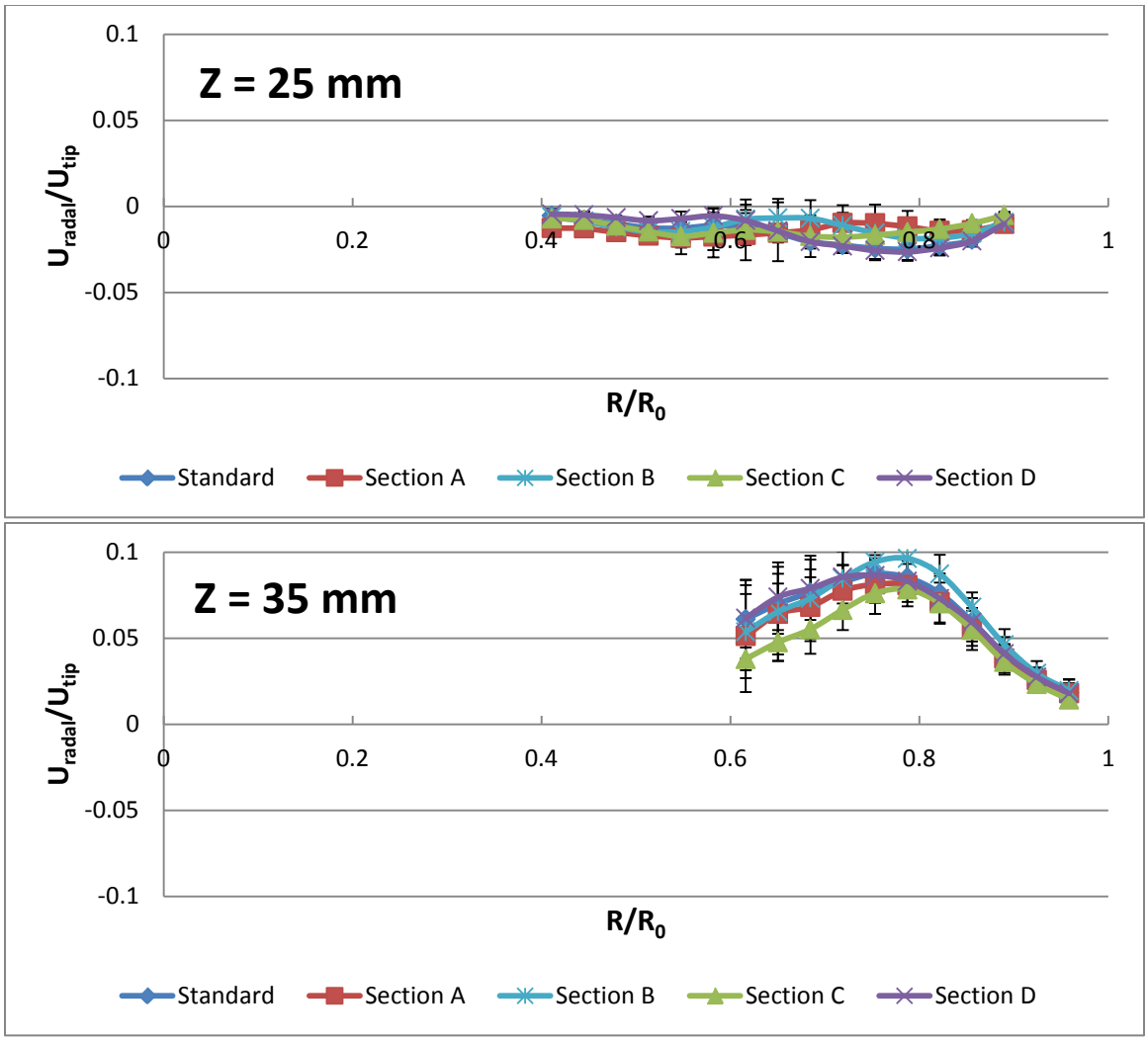

Figure 3.16 PIV measurements for radial velocities on different iso-surfaces around the impeller.

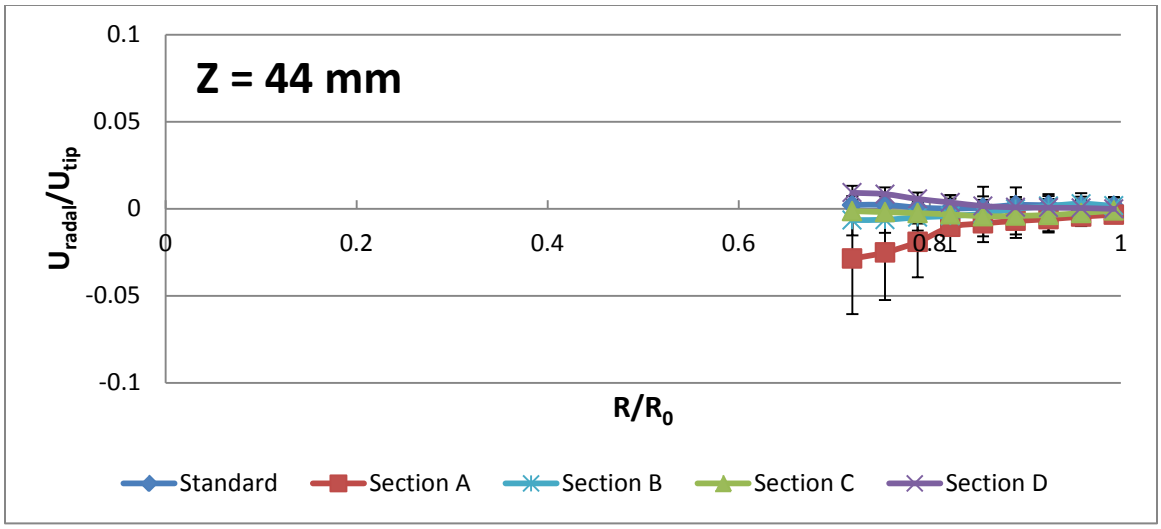

Figure 3.16 PIV measurements for radial velocities on different iso-surfaces around the impeller (Continued).

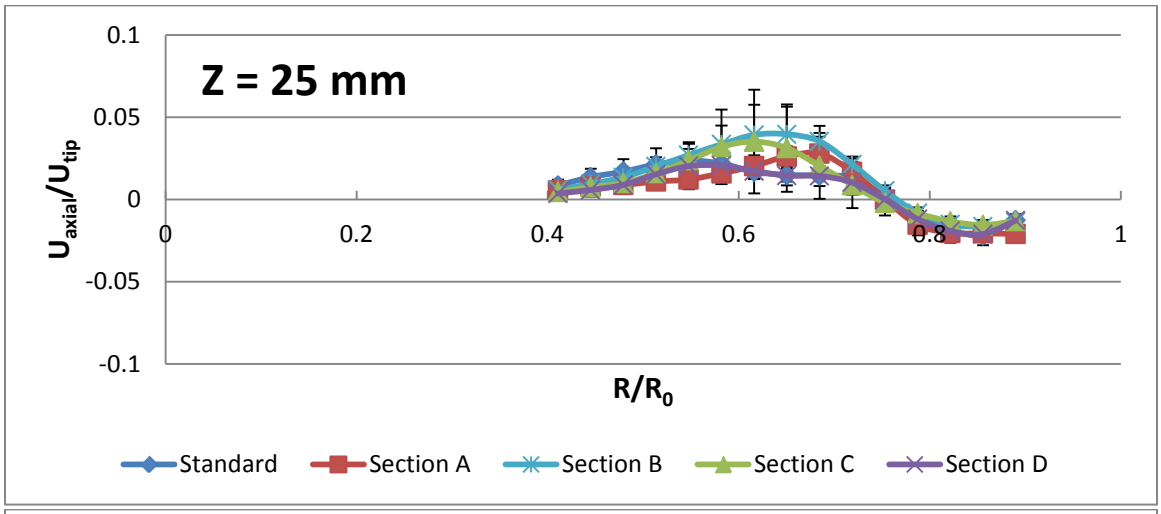

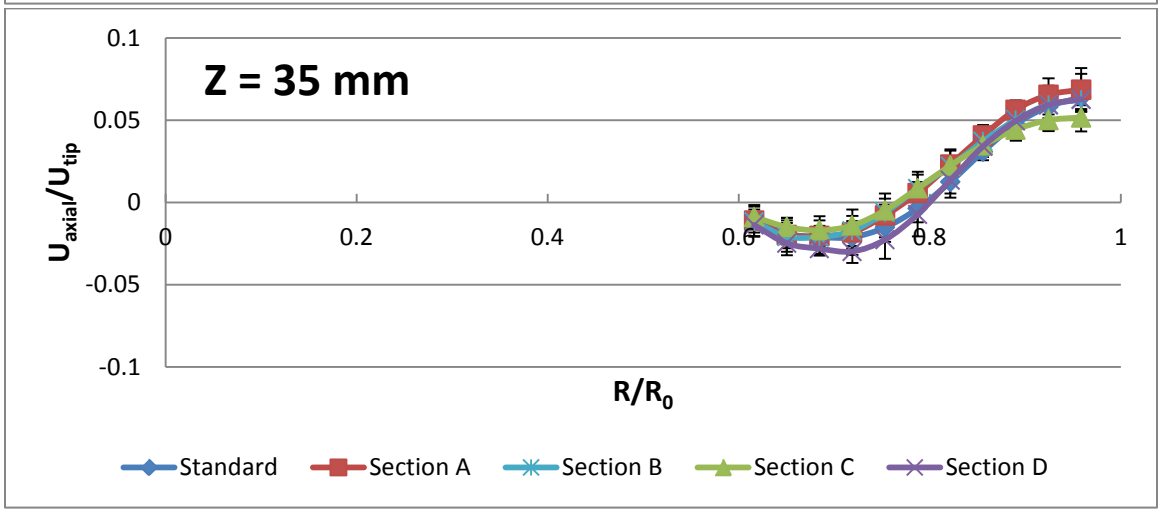

Figure 3.17 PIV measurements for axial velocities on different iso-surfaces around the impeller.

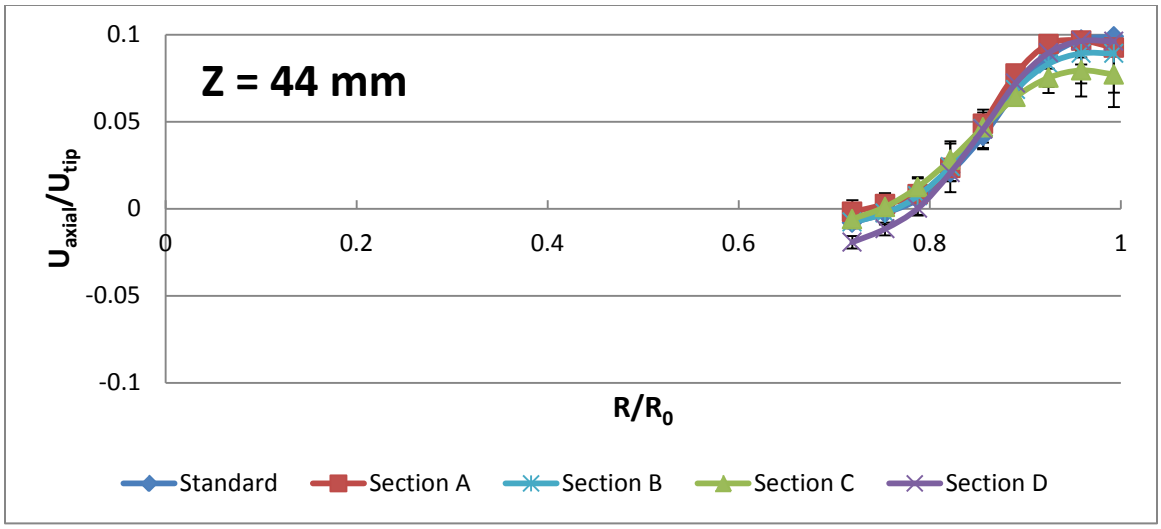

Figure 3.17 PIV measurements for axial velocities on different iso-surfaces around the impeller (Continued).

3.2.2.4 Velocity Profiles above the Impeller. Figure 3.18 and 3.19 show, respectively, the average radial and axial velocity profiles and standard deviation for each data point on the iso-surfaces above the impeller, i.e., Z=50 mm, 75 mm, 100 mm, and 125 mm. In section A, just part of the velocity profiles were shown in the figures, since the laser sheet was blocked by the cannula. The differences in velocities profiles between different systems can be easily observed in this region, specifically, in the area where the cannula was located, i.e., for ~0.7<R/R_0<~0.8 and in the downward recirculation zone, i.e., for ~0.3< R/R_0<~0.5. In the region where ~0.7<R/R_0<~0.8, the radial velocities in Section A were much higher than those in other sections on all iso-surfaces. The largest differences in axial velocities were in the region ~0.3< R/R_0<~0.5 where all the testing sections produced velocity profiles higher than those in in standard system. Overall, in Section A the impact of the cannula was most pronounced. Also the impact of the cannula continued in the region downstream of cannula, i.e., Section B, Section C, as well as Section D.

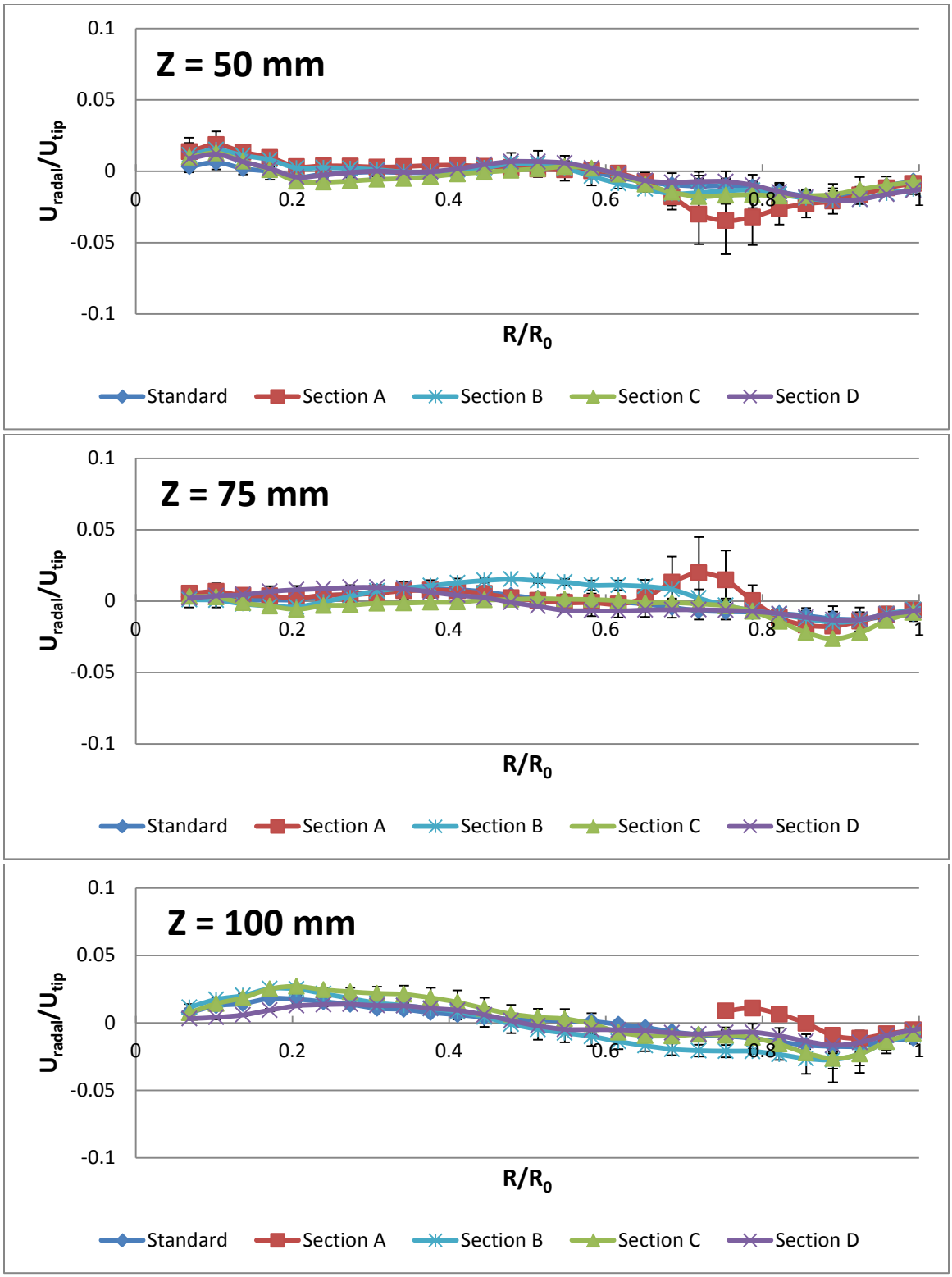

Figure 3.18 PIV measurements for radial velocities on different iso-surfaces around the impeller.

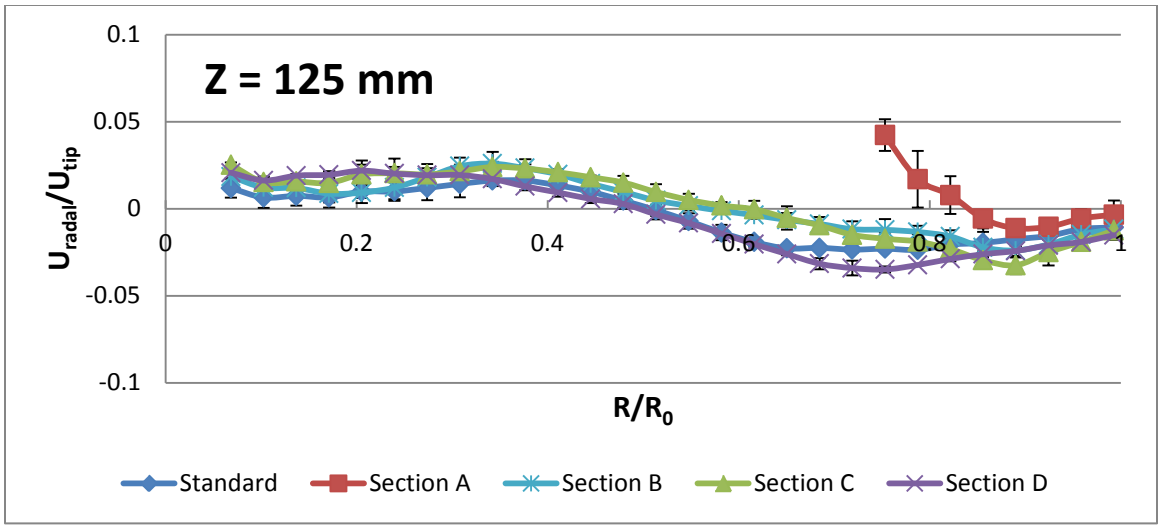

Figure 3.18 PIV measurements for radial velocities on different iso-surfaces around the impeller (Continued).

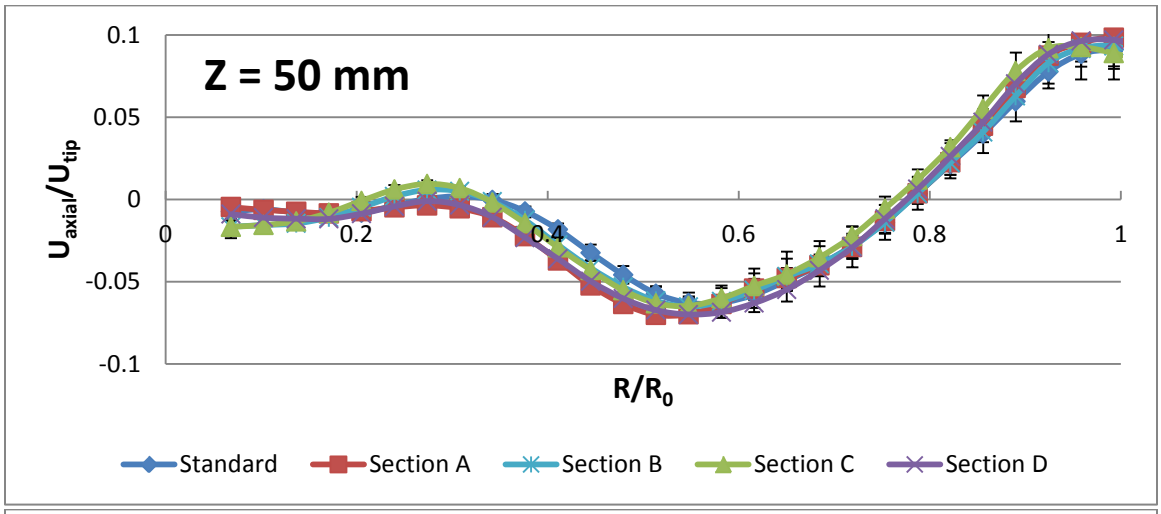

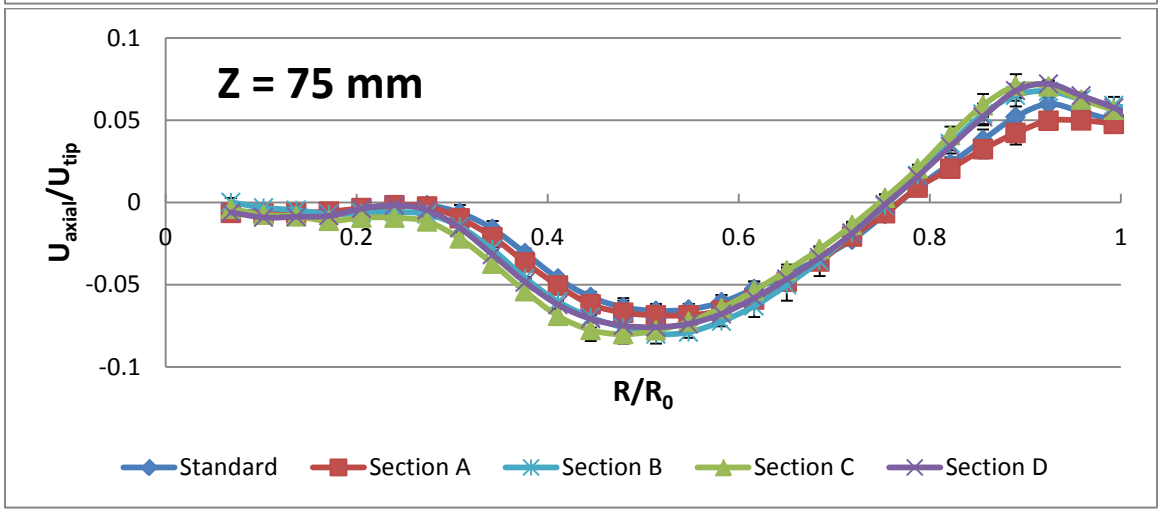

Figure 3.19 PIV measurements for axial velocities on different iso-surfaces around the impeller.

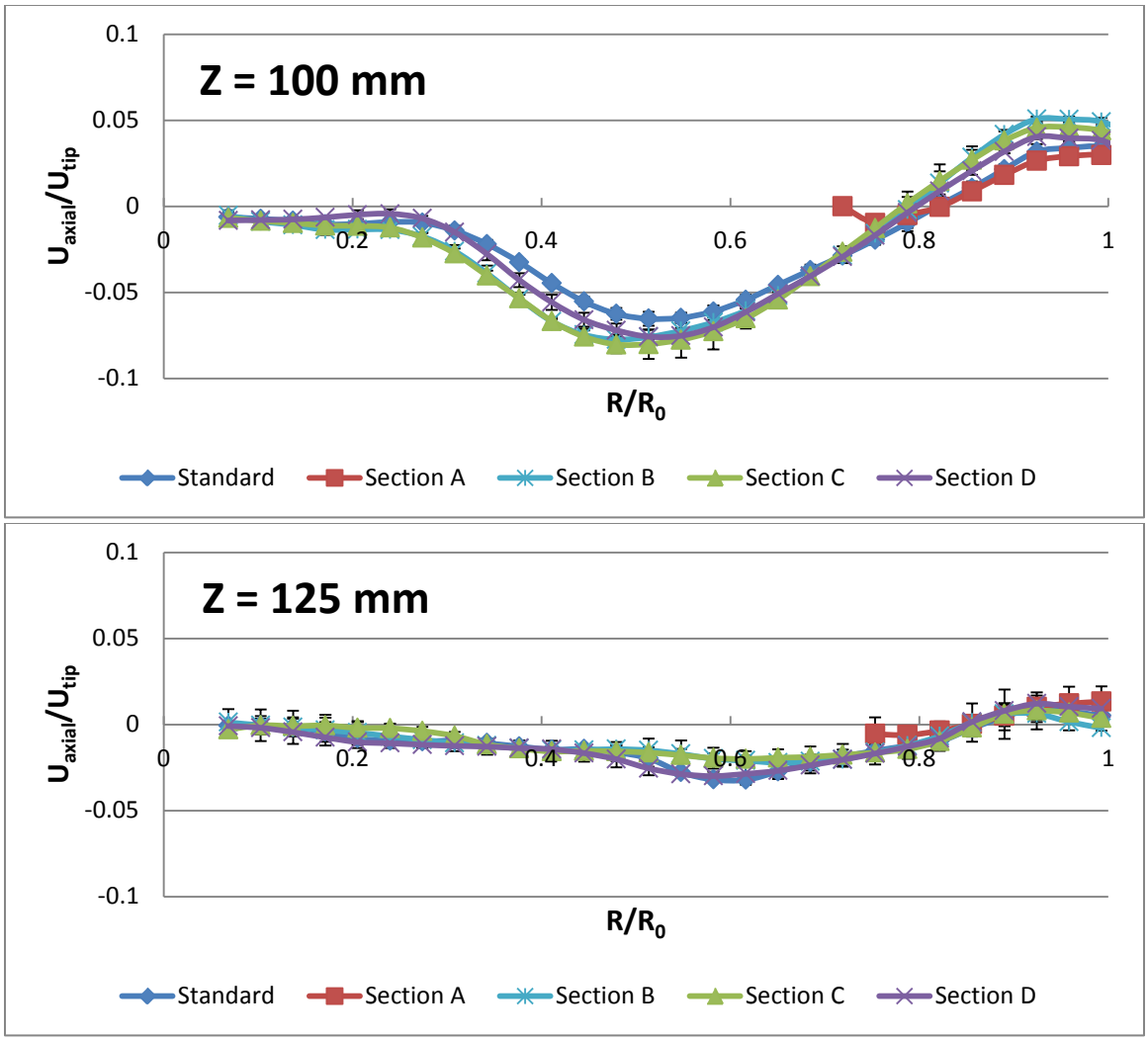

Figure 3.19 PIV measurements for axial velocities on different iso-surfaces around the impeller (Continued).

3.2.3 Sums of Squared Deviations of the Velocity Profiles

The sum of squared deviation (S value) was calculated for each of the three regions, as described in Section 2.2.2. The results are shown in Table 3.4.

Overall, the velocities in Section A had largest total deviations compared to those in the standard system than the other four sections in the system. This was followed by Section C and Section B. In the region above the impeller, the impact of the cannula was most pronounced, and Section A, Section B and Section C produced the similar

deviations and much higher than Section D. The velocities around the impeller didn't show the significant effect on the presence of the cannula, considering the highest standard deviation (0.006907) in all three regions in the reproducibility test. Section A also was where largest difference can be found in the region below the impeller. In this region, Section B, Section C and Section D produced similar but a lower S value, indicating the effect of cannula was not significant in these sections.

Table 3.4 Sums of Squared Deviations

Section	Section A	Section B	Section C	Section D
Below the Impeller	0.007977	0.002676	0.002578	0.002769
Around the Impeller	0.005403	0.003755	0.005377	0.001062
Above the Impeller	0.015841	0.012758	0.014871	0.006614
Total	0.029221	0.019189	0.022826	0.010445

CHAPTER 4

DISCUSSION

4.1 Dissolution Tests

In this work, the results of the dissolution experiments show that the dissolution profiles for the systems with cannulas tend to be higher than those in the standard systems, without cannulas irrespective of tablet position, with the exception of the tablet Position D2. These differences were slightly but observable from the averages of triplicated paired dissolution profiles (as reported in Figure 3.2 through Figure 3.10, with the exception of Figure 3.10), and ranged from 4.5% to 0.2%, depending on tablet location. Most differences between the dissolution profiles might not be attributed to data scatter since the average standard deviation of triplicate experiments was usually small (the standard system 1.38% and the testing system 1.18%). The Student's t-test values for all runs were lower than the 0.05 significance level by one or more orders of magnitudes, indicating that the systems with and without the cannula generated statistically different dissolution profiles, i.e., that the results obtained with the two systems were unlikely to come from the some population.

On the other hand, the difference factor f_1 and similarity factor f_2 for most runs were within the FDA required ranges, i.e., $0<f_1<15$ and $50<f_2<100$, indicating that the differences introduced by the permanently inserted cannula, although clearly measurable, were not typically significant enough to fail the dissolution test (although the f_1 test for Position A1 failed). However, the enhancing effect of the presence of the cannula on the dissolution rate would reduce the tolerance limit of the dissolution test and make the system with cannula permanently inserted more likely to fail the test. For example, a

tablet that would intrinsically dissolved slightly faster but still within the dissolution testing acceptance range if measured in a standard system, could possibly produce an out-of-range dissolution profile and fail the test due to the presence of the permanently inserted cannula enhancing the dissolution rate. Therefore, dissolution test developers should consider developing baseline dissolution profiles with the cannula always inserted in order to reduce the impact that any hydrodynamic changes associated with the presence of the cannula can introduce.

The effect of the presence of the cannula could be observed for both centered and off-center tablet locations (Table 3.2). On average, this impact was more significant for tablet closer to the center position. It is important to emphasize the dissolution profiles for centered tablets were appreciably affected by the presence of the cannula (Figure 3.2), and this is important in practice because this is the most likely tablet location in most practical situations. For tablets in the 10° off-center positions, the cannula effect was even more significant, but only for tablets positioned the nearest to the cannula (Position A1; Figure 3.3). For the tablets in the 20° off-center positions, a similar but reduced trend was observed by comparing the dissolution profiles for tablets at the same azimuthal location nearest to the cannula but at different off-center displacements, i.e., Position A1 (on the 10° circle; Figure 3.3) vs. Position A2 (on the 20° circle; Figure 3.7).

The reasons for such a small geometric change (the cannula OD was only 3.14 mm and the length immersed in the medium was 44.22 mm) could produce an appreciable effect on dissolution can be attributed to two different but related phenomena. The first is the presence of a small “baffle” introduced by the inserted cannula in the dissolution system. As a small symmetrical unbaffled system, the standard

USP Apparatus 2 generates a tangential flow with very limited velocity components in vertical and radial directions around the impeller and the shaft (Bai and Armenante, 2008; Bai et al., 2011, 2007; Baxter et al., 2005). The tangential flow would be partially affected by the cannula, just like any small baffle. A slightly stronger top-to-bottom recirculation could be produced in the system, resulting in the enhanced dissolution rate of the tables. This is not surprising because a number of mixing literature (Akiti et al., 2005; Armenante et al., 2005; Atiemo-Obeng et al., 2004) documents the effect of the introduction of baffles, even small baffles, on mixing.

The second effect is a small asymmetry introduced by the cannula inserted on one side of an otherwise symmetrical USP Apparatus 2 system. As a perfectly symmetrical system, Apparatus 2 can be expected to be very sensitive to any deviation from symmetry, such as the presence of the cannula. In general, asymmetric systems generate a non-symmetrical three-dimensional flow to enhance mixing effects. Loss of symmetry can result from a number of geometric irregularities and operating irregularities (Scott, 2005), such as a slightly geometry changes of the vessel (Tanaka et al., 2005; Liddell et al., 2007), small displacement of the impeller location or even the off-center location of the tablet (Bai and Armenante, 2009). In most cases, changes in the dissolution profiles even test failures have typically been reported for these systems.

The combined effects (baffle effect and asymmetry effect) can be especially important for the flow in the region below the impeller where the tablets are always located. Usually the flow in this zone is especially week and can be easily perturbed by even small changes in the system. When this happens, a tablet located in the same region

can experience a relative but appreciably more intense flow around it, thus resulting in a relative higher dissolution rate, as observed here for most tablet locations.

The tests conducted using the USP procedure, i.e., the dropping of the tablet in the vessel at the beginning of the test, confirmed that the cannula had an effect on dissolution. The dissolution profiles in the testing system were slightly higher than those in standard system not only when the average of three runs were considered, but also in each individual run.

As mentioned before, the cannula had a stronger effect on the 10° off-center locations than on the 20° positions by comparing the tablet position in the same azimuthal direction but on the different circles. The tablets on the center position were significantly affected. This implies that the hydrodynamic effect of the cannula is different depending on the tablet positions, and it is more pronounced when the tablets are closer to the center of the vessel bottom and in the zone where the cannula was located (Position A1 and Position A2).

4.2 PIV Measurements

The results of the PIV measurements were consistent with the results from experimental dissolution tests, and showed that the hydrodynamics in the dissolution vessel was slightly affected by the introduction of the cannula.

The general, the overall flow pattern in the dissolution vessel was similar in all four sections in the testing system, according to the velocity vector maps (Figure 3.12 and Figure 3.13). The main features of this flow consisted of two recirculation loops, below and above the impeller, and a very weak-velocity region below the shaft. On the other hand, when the cannula was inserted a significant flow perturbation was observed above

the impeller, and not only on Section A, i.e., in proximity of the cannula, but also in Section B and Section C. This confirmed that the cannula produce a “baffle effect” altering the fluid flow in the vessel. This effect decreased downstream of the cannula and was minor on Section D, the most downstream section with respect to the cannula location. The effect of the cannula could be even better noticed by comparing the velocities on Section A-Front and Section A-Back. The velocity increase in this region is ultimately responsible for the change in velocities in the lower portion of the vessel and the resulting increase in the dissolution rate of the tablets fixed in those positions, since tablets would directly experience the flow in this region.

Further quantitative study on the eleven iso-surfaces selected showed in detail the differences in the radial velocity profiles and axial velocity profiles between the standard system and the testing system, and between different sections in the testing system (Figures 3.14 through 3.19).

In the region above the impeller, the most significant difference was observed in Section A, and this was in agreement with the observation from the velocity vector maps. The S values in this region showed the results of the “baffle effect” and the largest S value was found in Section A. The cannula disturbed the flow in this section and generated the largest deviation in Section A, and then this flow perturbation extended downstream through Section B, Section C and became much weaker when passing through Section D. Much smaller S values were found in Section D, which was in agreement with the vector velocity map of Section D.

In the region around the impeller, despite the largest variation in the reproducibility test due to more turbulent flows (Table 3.3), the S values were relative

uniform in all four sections (Table 3.4), indicating that the introduction of the cannula did not significantly affect flows in this region, which remained dominated by the impeller.

The region below the impeller was more carefully studied and four iso-surfaces were selected here (i.e., Z=5 mm, 10 mm, 15 mm and 20 mm), since the dissolution rate of the tablet was expected to be more sensitive to the flow velocity it experienced directly in this region. Section A was found to have the largest S value of all the sections, which coincided with the faster dissolution rates of tablets in Position A1 and Position A2. This can be explained that the perturbation generated by the cannula above the impeller which reached the region below the impeller at a location nearest to the cannula. Although the perturbation may die down along the recirculation pattern, its effect could still be noticed, especially considering the low velocities baseline below the shaft. This also explained why the effect was more pronounced for tablets placed 10° off-center circle positions than 20° off-center circle. The tablet positions in the center and 10° circle were within or partially within the low velocity region under the impeller, while the 20° circle positions were within the upwards recirculation region. Therefore, the baseline velocities were much lower in central and 10° circle positions. As a result, any velocity perturbation in this region was more significant, and greater differences in dissolution rates between the two systems were observed for these tablet positions.

CHAPTER 5

CONCLUSIONS

The hydrodynamic effects of a cannula in USP Dissolution Testing Apparatus 2 were determined by experimentally comparing the dissolution profiles obtained in the testing system with those in the standard system, and by determining the flow velocities in the two systems via PIV.

Several conclusions can be drawn from this study. The cannula inserted in the USP-specified sampling zone in the USP Apparatus 2 resulted in dissolution profiles for non-disintegrating salicylic acid tablets located at different positions on the vessel bottom that were statistically different from the corresponding dissolution profiles obtained in the absence of the cannula, as indicated by the result of a paired t-test ($P(t\text{-test})<0.05$). These differences were reproducible and systematic: in nearly all cases, the presence of the cannula resulted in faster dissolution rates.

The magnitude of the difference between dissolution profiles depended on tablet location: larger differences were observed with tablets located closer to the cannula. These effects can be attributed to the changes in hydrodynamics introduced by the presence of the cannula, and mainly to the partial to the partial baffling effects and the loss of symmetry caused by the insertion of the cannula.

The PIV measurements showed that the cannula did have a baffling effect on the hydrodynamics in the dissolution vessel. This effect resulted in slightly changes in the velocities in the vessel, and therefore in slightly larger differences in the dissolution rate of the testing tablets. The baffling effect was clearly observed in the region where the cannula was inserted. The flow perturbation that it generated became gradually weaker

downstream of the agitation path. This perturbation was also found to reach the region below the impeller but only the section nearest to the cannula had significant higher fluid velocities. Additionally, the PIV results showed that the baffle effect was not strong enough to break the overall flow pattern, or to affect the region around the impeller, which was dominated by the agitation flow.

In summary, the hydrodynamic effects generated by the cannula are real and observable, resulting in slightly modification of the fluid flow in the dissolution vessel and therefore in detectable differences in the dissolution profiles. Although the differences between the dissolution profiles in two systems were generally small enough for the dissolution profiles to be considered acceptable using the FDA criteria (f_1 and f_2 values), the enhanced dissolution rate caused by the cannula could reduce the tolerance limit of the dissolution test and make tablets tested in systems with a cannula permanently inserted more likely to fail the test. Therefore, it is recommended that dissolution test developers who plan to conduct manual sampling with the cannula inserted permanently should develop baseline dissolution profiles with a cannula always inserted, in order to reduce the impact that any hydrodynamic changes associated with the presence of the cannula can introduce.

REFERENCES

Akiti O., Yeboah A., Bai G., Armenante P.M., 2005. Hydrodynamic effects on mixing and competitive reactions in laboratory reactors. Chem. Eng. Sci. 60, 2341-2354.

Atiemo-Obeng VA, Penney WR, Armenante, PM. 2004. Solid-Liquid Mixing, in Handbook of Industrial Mixing-Science and Practice, by Paul, E. L., Atiemo-Obeng, V. A., and Kresta, S. M. (editors), pp. 543-584, John Wiley & Sons, New York.

Bai G, Armenante P.M., Plank R.V., Gentzler M., Ford, K., Harmon P., 2007. Hydrodynamic investigation of USP dissolution test apparatus II. J. Pharm. Sci. 96, 2327–2349.

Bai G., Armenante P. M. 2008. Velocity distribution and shear rate variability resulting from changes in the impeller location in the USP dissolution testing apparatus II. Pharm Res 25, 320-336.

Bai G., Wang Y., Armenante P. M. 2011. Velocity profiles and shear rate variability in the USP Dissolution Testing apparatus 2 at different impeller agitation speeds. Inter J Pharmaceutics, 403, 1-14.

Bai, G., Armenante, P.M., 2009. Hydrodynamic, mass transfer, and dissolution effects induced by tablet location during dissolution testing. J. Pharm. Sci. 98, 1511-1531.

Baxter, J.L., Kukura, J., Muzzio, F.J., 2005. Hydrodynamics-induced Variability in the USP Apparatus II Dissolution Test. Int. J. Pharm. 292, 17-28.

Bocanegra, L.M., Morris, G.J., Jurewicz, J.T., Mauger, J.W., 1990. Fluid and particle laser Doppler velocity measurements and mass transfer predictions for USP paddle method dissolution apparatus. Drug Dev. Ind. Pharm. 16, 1441-1464.

Bynum, K., Roinestad, K., Kassis, A., Pocreva, J., Gehrlein, L., Cheng, F., Palermo, P., 2001. Analytical Performance of a Fiber Optic Probe Dissolution System. Dissol. Technol. 8, 1–8.

Cohen, J.L., Hubert, B.B., Leeson, L.J., Rhodes, C.T., Robinson, J.R., Roseman, T.J., Shelter, E., 1990. The Development of USP Dissolution and Drug Release Standards. Pharm. Res. 7, 983-987.

Costa, P., Lobo, J.M.S., 2001. Modeling and comparison of dissolution profiles. Eur. J. Pharm. Sci. 13, 123-133.

Cox, D.C., Furman, W. B, Moore, T. W. and Wells, C. E., 1984. Guidelines for Dissolution Testing: An Addendum," Pharm. Technol. 8, 42-46.

Cox, D.C., Furman, W.B., 1982. Systematic error associated with Apparatus 2 of the USP dissolution test I: effects of physical alignment of the dissolution apparatus. J. Pharm. Sci. 71,451-452.

Cox, D.C., Furman, W.B., Thornton, L.K., 1983. Systematic error associated with Apparatus 2 of the USP Dissolution Test III: limitation of calibrators and the USP suitability test. J. Pharm. Sci. 72,910-913.

Dantec Dynamics Inc FlowMap, 2000. PIV Installation & User's guide.

Gao Z, Moore T.W., Doub W.H., Westenberger BJ, Bushe L.F., 2006. Effect of deaeration methods on dissolution test in aqueous media: A study using a total dissolved gas pressure meter. J. Pharm. Sci. 95, 1606-1613.

Gao Z., Moore T.W., Doub W.H., 2008. Vibration effects on dissolution test with USP apparatus 1 and 2. J. Pharm. Sci. 97, 3335-3343.

Kukura, J., arratia, P.C., Szalai, E.S., Muzzio, F.J., 2003. Engineering tools for understanding hydrodynamics of dissolution tests. Drug Dev. Ind. Pharm. 29, 231-239.

Kukura, J., Baxter, J.L., Muzzio, F. J., 2004. Shear distribution and variability in the USP Apparatus 2 under turbulent conditions. Int. J.Pharm. 279,9-17.

Lapin, L. Statistics. Harcourt, Brace Jovannovich, Inc. New York, 1975.

Liddell M.R., Deng G., Hauck W.W., Brown W.E., Wahab S.Z., Manning R.G., 2007. Evaluation of glass dissolution vessel dimensions and irregularities. Dissolution Technol. 14, 28-33.

Lu. X., Lozano, R., Shah, P., 2003. In-Situ Dissolution Testing Using Different UV Fiber Optic Probes and Instruments. Dissol. Technol. 10, 6-15.

Mauger, J., ballard, J., Brockson, R., De, S., Gray, V., Robinson, D., 2003. Intrinsic dissolution performance of the USP dissolution apparatus 2 (rotating paddle) using modified salicylic acid calibration tablets: proof of principle. Dissol. Technol. 10, 6-15.

McCarthy, L, Kosiol, C., Healy, A.M., Bradley, G., Sexton, J., Corrigan, O., 2003. Simulating the hydrodynamic conditions in the United States pharmacopeias paddle dissolution apparatus. AAPS Pharm. Sci. Technol. 4.

McCarthy, L., Bradley, G., Sexton, J., Corrigan, O., Healy, A.M., 2004. Computational fluid dynamics modeling of the paddle dissolution apparatus: agitation rate mixing patterns and fluid velocities. AAPS Pharm. Sci. Technol. 5.

Mirza, T., Liu, Q., Vivilecchia, R., Joshi, Y., 2009. Comprehensive Validation Scheme for In Situ Fiber Optics Dissolution Method for Pharmaceutical Drug Product Testing. J. Pharm. Sci. 98, 1086-1094.

Moore, J.W. and Flanner, H.H. Mathematical Comparison of curves with an emphasis on in vitro dissolution profiles. Pharm. Tech. 1996, 20, 64-74.

Moore, T.W., 1996. Dissolution Testing: A Fast, Efficient Procedure for Degassing Dissolution Medium. Dissol. Technol. 3, 3-5.

Moore, T.W., Hamilton, J.F., Kerner, C.M., 1995. Dissolution testing: Limitation of USP prednisone and salicylic acid calibrator tablets. Pharmacopeial Forum 21, 1387-1396.

Nie, K., Li, L., Li, X., Zhang, Y., Mu, X., and Chen, J. 2009. Monitoring Ambroxol Hydrochloride Sustained-Release Tablets Release by Fiber-Optic Drug Dissolution In Situ Test System. Dissol. Technol. 16, 14-17.

Qureshi, S.A, Shabnam, J., 2001. Cause of high variability in drug dissolution testing and its impact on setting tolerances. Eur. J. Pharm. Sci. 12,271-276.

Qureshi, S.A., McGilveray, I.J., 1999. Typical variability in drug dissolution testing: study with USP and FDA calibrator tablets ad a marketed drug (glibenclamide) product. Eur. J. Pharm. Sci. 7, 249-258.

Savage, T. S. and Wells, C. S., 1982. Automated Sampling of In Vitro Dissolution Medium: Effect of Sampling Probes on Dissolution Rate of Prednisone Tablets, J. Pharm. Sci. 71, 670-673.

Schatz, C., Ulmschneider, M., Altermatt, R., Marrer, S., 2000. Manual In Situ Fiber Optic Dissolution Analysis in Quality Control. Dissol. Technol. 7, 6-13.

Scott P. 2005. Geometric Irregularities Common to the Dissolution Vessel. Dissolution Technol 12, 18-21

Tanaka, M., Fujiwara, H., Fujiwara, M. 2005. Effect of the Irregular Inner Shape of a Glass Vessel on Prednisone Dissolution Results. Dissol. Technol. 12, 15-19.

The United States Pharmacopeia & The National Formulary. 2012. The Official Compendia of Standards, USP 35-NF 30. The United States Pharmacopeial Convention, Inc., Rockville, Maryland.

US Food and Drug Administration, Center for Drug Evaluation and Research (CDER). 1997. Guidance for Industry - Dissolution Testing of Immediate Release Solid Oral Dosage Forms.

Wang, Y. and Armenante, P. M., 2012. A Novel Off-center Paddle Impeller (OPI) Dissolution Testing System for Reproducible Dissolution Testing of Solid Dosage Forms," J. Pharm. Sci., 101, 746-760.

Wells C. 1981. Effect of Sampling Probe on Dissolution of Tableted Drug Samples. J. Pharm. Sci. 70, 232-233.